

AD-780 629

**SYNERGISTIC DAMAGE CAUSED BY MULTIPLE  
FRAGMENT IMPACT ON CLOSED SYSTEMS**

**Russell T. Boice, Jr.**

**Air Force Institute of Technology  
Wright-Patterson Air Force Base, Ohio**

**March 1974**

**DISTRIBUTED BY:**

**NTIS**

**National Technical Information Service  
U. S. DEPARTMENT OF COMMERCE  
5285 Port Royal Road, Springfield Va. 22151**

REPORT DOCUMENTATION PAGE		READ INSTRUCTIONS BEFORE COMPLETING FORM
1. REPORT NUMBER GAW/MC/10	2. GOVT ACCESSION NO.	3. RECIPIENT'S CATALOG NUMBER <b>AD-780629</b>
4. TITLE (and Subtitle) Synergistic Damage Caused by Multiple Fragment Impact on Closed Systems		5. TYPE OF REPORT & PERIOD COVERED AFIT Thesis
7. AUTHOR(s) Russell T Boice Jr		6. PERFORMING ORG. REPORT NUMBER
9. PERFORMING ORGANIZATION NAME AND ADDRESS Air Force Institute of Technology (AFIT-EN) Wright-Patterson AFB, Ohio 45433		8. CONTRACT OR GRANT NUMBER(s)
11. CONTROLLING OFFICE NAME AND ADDRESS Air Force Armament Development and Test Center Wright-Patterson AFB, Ohio 45433		10. PROGRAM ELEMENT, PROJECT, TASK AREA & WORK UNIT NUMBERS
14. MONITORING AGENCY NAME & ADDRESS (if different from Controlling Office)		12. REPORT DATE March 1974
		13. NUMBER OF PAGES 76
		15. SECURITY CLASS. (of this report) Unclassified
		15a. DECLASSIFICATION DOWNGRADING SCHEDULE
16. DISTRIBUTION STATEMENT (of this Report) Approved for public release; distribution unlimited.		
17. DISTRIBUTION STATEMENT (of the abstract entered in Block 20, if different from Report)		
18. SUPPLEMENTARY NOTES Approved for public release; IAW AFR 190-17.  JERRY C. HIX, Captain, USAF Director of Information		
19. KEY WORDS (Continue on reverse side if necessary and identify by block number) Penetration mechanics Post-perforation effects Al-Al impact system Vaporifics; -Aluminum combustion in impact  Reproduced by NATIONAL TECHNICAL INFORMATION SERVICE U. S. Department of Commerce Springfield VA 22151		
20. ABSTRACT (Continue on reverse side if necessary and identify by block number) The purpose of this study was to hypothesize the most probable cause for synergistic damage effects sometimes observed when multiple aluminum fragments impact an aluminum box structure. The synergistic damage is characterized by an unexpected increase of pressure within		

Unclassified

SECURITY CLASSIFICATION OF THIS PAGE(When Data Entered)

Block 20.

the box causing notable bulging. There are reports of a sudden pressure increase at approximately 8000 ft/sec. The study was conducted through literature search and simple engineering approximations.

The study concentrated on physical phenomena associated with an impact velocity of approximately 8000 ft/sec. Heyda's plug-shattering model was adapted to show that under certain impact geometry conditions that numerous micro-sized fragments could be released into the closed system, at or above the impact velocity. At approximately 8000 ft/sec these micro-sized fragments encounter stagnation temperatures slightly greater than the melting point of aluminum oxide, 2300 K. At this velocity, the stagnation heating begins to cause oxygen in the air to dissociate to atomic oxygen, a very aggressive oxidizer. These conditions are compared to existing experimental evidence to show that there is a strong likelihood that the secondary fragments would ignite and burn almost instantly releasing, for a multiple impact case, a significant amount of energy into the system.

The Heyda plug-shattering model was extended to spherical projectiles. Graphs for the application of the model to other than aluminum-aluminum systems are provided.

It is recommended that further experimental confirmation of the predictability of the synergistic damage phenomenon be performed before direct application is attempted.

Unclassified

SECURITY CLASSIFICATION OF THIS PAGE(When Data Entered)

SYNERGISTIC DAMAGE CAUSED BY MULTIPLE  
FRAGMENT IMPACT ON CLOSED SYSTEMS

GAW/MC/74-10

Russell T. Boice, Jr  
Lt Col USAF

Approved for public release; distribu-  
tion unlimited.



**SYNERGISTIC DAMAGE CAUSED BY MULTIPLE  
FRAGMENT IMPACT ON CLOSED SYSTEMS**

**THESIS**

**Presented to the Faculty of the School of Engineering  
of the Air Force Institute of Technology**

**Air University**

**in Partial Fulfillment of the  
Requirements for the Degree of**

**Master of Science**

**by**

**RUSSELL T. BOICE, JR    B.S.M.E.  
LT COL                            USAF**

**Graduate Air Weapons**

**March 1974**

**Approved for public release; distribution unlimited.**

Preface

While visiting the Air Force Armament Laboratory (AFATL) in the Spring of 1973, the results of an experiment were presented in an overview briefing. The first picture was that of an aluminum box-like structure that showed damage in the form of multiple punctures in both the front and back surfaces. A few cracks were observed, but the box was intact. A second picture of a similar box was shown. This box was more severely damaged; there were large cracks and evidence of bulging of both the front and back faces. The difference between the two events was that the first box had been subjected to multiple steel fragments; the second box had been subjected to multiple aluminum fragments. Evidently there was a mechanism working on the Al-Al system that was not present in the steel-Al system.

Subsequent conversations with AFATL personnel indicated that there appeared to be a "magic number" for the Al-Al system - 8000 ft/sec impact velocity and that similar behavior had been observed with other materials impacting Al structure. The cause of the synergistic damage mechanism was not understood.

The purpose of this study was then to present a reasonable case for the cause of the synergistic damage by focusing on the "magic number" - 8000 ft/sec. I must express my thanks to the faculty and students of the Graduate Air Weapons class as they patiently listened to dozens of hypotheses--and

explanations why that hypothesis wouldn't apply. Especially my thanks to my advisory committee, Dr Peter J. Torvik, Maj Louis Montulli and Capt Wesley Crow who bore the brunt of these discussions.

RTB

<i>Abstract</i>	<u>Contents</u>	
Preface . . . . .		i 11
List of Figures . . . . .		vi
 I. Introduction. . . . .		 1
Purpose and Scope. . . . .		1
Background . . . . .		1
Approach . . . . .		3
 II. Factors Contributing to Synergistic Damage. . .		 5
Multiple Fragment Impact . . . . .		5
Energy Release Due to Particle Ablation. . .		7
Heyda Plug-Shattering Model. . . . .		12
Extrapolation of the Heyda Plug-Shattering Model to Spherical Projectiles . . . . .		19
Aerothermodynamic Effects on Secondary Fragments. . . . .		23
Fragment Heating . . . . .		24
Effects on Ambient Atmosphere Surround- ing Fragments. . . . .		27
Combustion and Ignition of Aluminum Fragments. . . . .		31
Summary of Damage Mechanism. . . . .		40
 III. Design Considerations . . . . .		 41
Plug-Shattering for Other Than Al-Al Impacts. . . . .		41
Pressure Increase in a Closed System . . . .		44
Other Design Considerations. . . . .		46
 IV. Conclusions and Recommendations . . . . .		 48
Cause of Synergistic Damage Mechanism. . . .		48
Application of the Synergistic Damage Mechanism. . . . .		49
Future Activity. . . . .		50
 Appendix A: Sample Calculations . . . . .		 52
Application of Heyda Plug-Shattering Model for Calculation of Impact Velocity for Incipient Shattering . . . . .		53
Prediction of Incipient Shattering by Heyda Plug-Shattering Model for a Spherical Pro- jectile. . . . .		54

Appendix B: Charts Required for Application of The Heyda Plug-Shattering Model . . . . .	56
Bibliography. . . . .	63
Vita. . . . .	65

List of Figures

Figure		Page
1	Composite of Several Sources Representing Pressure Increases in a Closed Box as the Impact Energy Increases. There are occasional reports of sudden pressure increase around 8000 ft/sec. . . . .	3
2	Ablation of Al Particle at High Velocity (10,800 ft/sec). Clearly Shows Effect of Decreasing Particle Size on Energy Deposition . . . . .	11
3	Geometry and Nomenclature for Development of Heyda Plug-Shattering Model . . . . .	13
4	Plot of Dimensionless Variable S Versus the Ratio of Material Density Before Impact to Density After Impact. Additional Plots for a Wide Variety of Materials are Shown in Appendix B. . . . .	15
5	Case Where $S < \frac{T}{R}$ . Energy is Deposited at Plug Centerline at an Explosive Rate. . . .	17
6	Geometry of Spherical Projectile Impacting Plate for Extension of Heyda Plug-Shattering Model . . . . .	20
7	Ballistic Limit Curves; $t_2$ is Thickness of Witness Plate . . . . .	21
8	Temperature Behind Hypersonic Shock . . . . .	25
9	Stagnation Temperature for a Circular Cylinder . . . . .	26
10	Stagnation Point Heat Transfer in Laminar Equilibrium Dissociated Flow . . . . .	27
11	Pressure Increase Across Shock Wave for a Right Cylindrical Body at Hypersonic Velocities . . . . .	28
12	Stagnation Pressure at Leading Edge of a Right Cylinder at Hypersonic Velocities. . .	29
13	Chemical Effects of Air at Various	

Figure		Page
	Velocities and Altitudes. . . . .	30
14	Compressibility Factor for Air. . . . .	31
15	Experimental Ignition and Fragmenta- tion Limits ( $35\mu$ Diameter Aluminum). . . . .	33
16	Ignition Time for $70\mu$ Al Particles in High Temperature Air . . . . .	34
17	Burning Time of Al Fragments as Function of Particle Size and Activity of Oxidizing Atmosphere. . . . .	35
18	Burning Time of Al Particles as Function of Activity. $Q_k^r$ Repre- sents Concentration and Availability of Free Oxygen, Increasing $a_k^r$ Implies Greater Activity . . . . .	36
19	Partial Pressure of Atomic Oxygen as a Function of Particle Velocity, Calculated from Eqn 31 and Fig 8 . . . . .	39
20	Velocity Required for Al and Steel Projectiles at Incipient Plug- Shattering . . . . .	42
21	Pressure Change per Milligram of Al Oxidized in a One Cubic Foot Volume . . . . .	46

## I. Introduction

### Purpose and Scope

The purpose of this study was to hypothesize the most probable cause for synergistic damage effects observed when multiple aluminum fragments impact a box-like aluminum structure with a velocity range of 2-5 km/sec. The study was conducted through literature search and simple engineering approximations. No experimental verification was contemplated since the Air Force Armament Laboratory (AFATL) would be conducting a similar study based on a comprehensive test program. Simple engineering design data criteria were to be tentatively established for the Al-Al system and some extension made for other materials.

### Background

In the late 1940's it was observed that when high velocity fragments perforate the skin and internal structure of an aircraft, flashes or semi-explosions occur which may cause considerable bulging and tearing. The physical nature of the phenomenon was attributed to burning of aluminum particles, the source of which was not specified (Ref 1:1).

During the 1960's investigations of hypervelocity meteorite impacts, several investigators reported significant impact flash when aluminum impacted aluminum plates, especially at velocities greater than 12,000 ft/sec with an air or oxygen atmosphere behind the plate. The impact flash was

generally attributed to the burning of the secondary particles of aluminum (Ref 2,3).

Backman and Stronge reported on a careful investigation of the Al-Al impact system but were unable to show a significant contribution to pressure inside of a box by combustion of Al in air. They show a general correlation between pressure and the kinetic energy of the impacting system (Ref 4).

More recently, work sponsored by AFATL has shown a significant synergistic damage mechanism when multiple steel fragments impact box-like Al structures. The velocity of the impacting fragments was in the range of 4000-8000 ft/sec.<sup>1</sup>

Unpublished information from AFATL<sup>2</sup> indicates that at an impact velocity of approximately 8000 ft/sec, for some conditions, a significant sudden pressure increase can be observed.

---

<sup>1</sup> Extracted from unclassified portion of a classified document. For specifics contact School of Engineering (ENE) Air Force Institute of Technology, Wright-Patterson AFB, Oh 45433.

<sup>2</sup> Conversation with Dr. McArdle, AFATL/DLRD, March 1973.

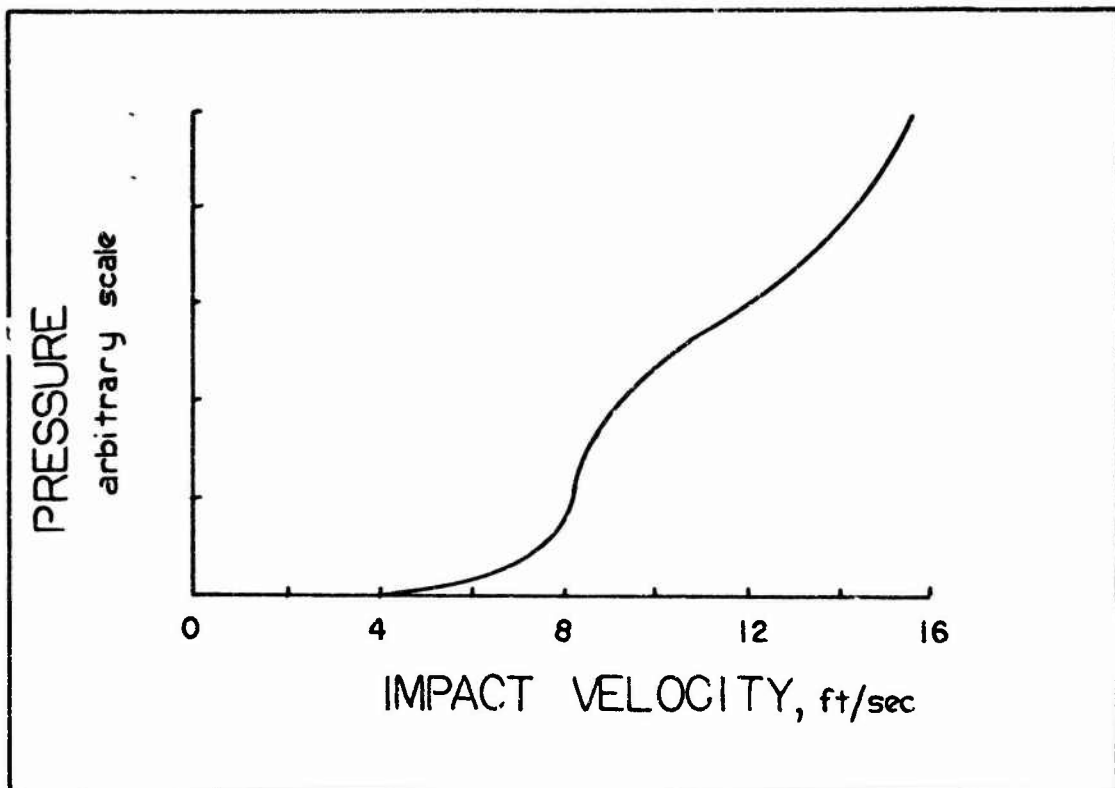


Fig 1. Composite of several sources representing pressure increases in a closed box as the impact energy increases. There are occasional reports of sudden pressure increase around 8000 ft/sec.

#### Approach

At least two observers have reported a sudden increase of pressure or impulse for a multiple fragment impact velocity of 8000 ft/sec. By understanding the phenomena associated with an 8000 ft/sec impact, one would be able to deduce a physical explanation for the synergistic damage effects on a closed system.

First, the effect of multiple-fragment impact was considered.

Second, to understand the parameters which would affect the pressure increase with impacting kinetic energy, a simple

drag model for the post-perforation fragments was considered.

Third, a source of high-energy secondary fragments was determined by a plug-shattering model by Heyda (Ref 6).

Finally, the aerothermodynamic and chemical effects on the high velocity secondary fragments was considered.

Throughout the study, factors which would influence design were observed.

## II. Factors Contributing To Synergistic Damage

This section will summarize the significant substudies which lead directly to an explanation of the damage mechanism. Many other factors were considered, of course, but are not reported either because it was believed that they would lead to an insignificant contribution or the complex interactions would obscure the basic phenomena.

### Multiple Fragment Impact

The first exercise was to construct a simple computer model which would provide an understanding of what areal density of fragments that would produce significant interactions. Visual evidence of ruptured plates has indicated large tears and evidence of tension failure in addition to a number of perforations when the synergistic damage was observed.<sup>3</sup> For this reason circumferential stresses were considered more important. The model was constructed as follows.

Consider several holes of radius  $a$  which are punched out of an infinite plate. Stresses of magnitude  $\sigma_c$  are generated at the edge of each hole by a fragment punching the hole. Assume also that the stresses at any distance  $r$  from the center of the hole is given by

$$\sigma_c = \sigma_0 \left( \frac{r}{a} \right)^{-n} \quad (1)$$

<sup>3</sup>See Footnote 1.

where  $\sigma_c$  is some critical circumferential stress  
 which will cause failure of the plate  
 $n$  is a dissipative parameter. For this model  
 $n$  is at least 2.

Now assume that more than one hole is punched at virtually the same time. The stress at any point was assumed to the summation of the stress emanating from each hole. The results of the analysis indicate that for more than a few hole diameter spacing, the interaction between punctures is negligible.

While this analysis is extremely simple, it is also very conservative. Since stresses are tensors and therefore have a directional property, they do not add directly except on the line joining the centers of each hole. Miklowitz' very much more elaborate and accurate analysis of the stresses induced by a punched hole indicated that the more rapidly the hole is punched the faster the stresses dissipated (Ref 5). Rinehart and Pearson (Ref 6) indicate that with impact velocities above 2000 ft/sec the shear stresses at the edge of the hole are negligibly small since the shear stresses act more like hydrodynamic stresses.

Therefore one can reasonably conclude that except for very closely spaced multiple impacts the increased damage effects are probably not due to additive or synergistic effects between multiple fragment impacts. Since the evidence indicates there is a much greater chance of observing the sudden pressure build-up for multiple fragment

impacts, there must be some other phenomenon which more probably occurs because of the many simultaneous impacts. It will be shown below that for certain fragment sizes and plate thicknesses one could get a planar shock in the plate which will produce numerous, high velocity, secondary micro-size particles.

#### Energy Release Due to Particle Ablation

Consider now the high velocity secondary particles leaving the impacting fragment-plate system into a closed system, the box. Considerable attention will be given to the source, size and velocities of these particles in a later section. At this time interest should be focused on Backman's observation that the pressure in a box increases with the kinetic energy of the impacting fragment and to the frequently observed post-perforation flash. In addition to the direct mechanical effects of the impact causing the pressure rise, these particles are being subjected to aerodynamic heating which may cause some of the aluminum particles to ablate, depositing energy in the form of heat in the closed system.

The following development is after Backman (Ref 4:32).

An energy balance on the  $i^{\text{th}}$  particle gives

$$q_i S = \dot{Q} \quad (2)$$

where  $q_i$  is the heat flux incident on the particle per unit area.

$S$  is the cross sectional area of the particle.

$\dot{Q}$  is the energy being carried away by the melting material per unit time.

The incident heat flux is equal to the stagnation pressure times the current velocity

$$q_i = \frac{1}{2} \rho_g V^3 \quad (3)$$

where  $\rho_g$  is the ambient gas density

$V$  is the current velocity of the particle.

For a particle of diameter  $D$  the rate of energy deposited is

$$q_i S = C_g \frac{\pi}{8} \rho_g V^3 D^2 \quad (4)$$

where  $C_g$  is a heat exchange coefficient.

The heat being carried away by melting  $\dot{Q}$  is given by

$$\dot{Q} = \dot{m} [C_p (T_m - T_o) + h_f] \quad (5)$$

where  $\dot{m}$  is the mass of material being carried away from the fragment per unit time

$C_p$  is the specific heat of the material

$T_m$  the melting temperature

$T_o$  the initial fragment temperature.

$h_f$  is the heat of fusion.

Equating the incident heat to the energy being carried away and solving for  $\dot{m}$ ,

$$\dot{m} = \frac{\pi C_g \rho_g D^2 V^3}{8 (C_p T + h_f)} \quad (6)$$

where  $T$  is equal to  $(T_m - T_o)$ .

Letting  $\dot{m} = \frac{dm}{dt}$ , changing variable of integration to distance traveled  $X$  rather than time, we have

$$dm = \frac{\pi C_g \rho_g V^2 D^2}{8 (C_p T + h_f)} dx \quad (7)$$

To integrate Eqn (7) an expression for  $V(x)$  is required. If the only drag forces are acting on the particle in the  $x$ -direction, Newton's second law gives

$$M_p \ddot{X} = - \frac{\pi}{8} \rho_g V^2 C_D D^2 \quad (8)$$

where  $C_D$  is the drag coefficient

$M_p$  is the mass of the fragment

$\ddot{X}$  is the second time derivative of distance.

Again, changing variables and integrating

$$V(x) = V_o \exp \left[ - \frac{\pi \rho_g D^2 C_D x}{8 M_p} \right] \quad (9)$$

Substituting (9) into (7),

$$dm = \frac{\pi C_g \rho_g D^2 V_o^2}{8 (C_p T + h_f)} \exp \left[ - \frac{\pi \rho_g D^2 C_D x}{4 M_p} \right] dx \quad (10)$$

Integrating, the mass  $\Delta m$  which is transferred from the rapidly moving, and decelerating particle, to the closed system in a distance  $\Delta S$  is given by

$$\Delta m = \frac{C_g V_o^2 m_p}{C_D (C_p T + h_f)} \left[ 1 - \exp \left( - \frac{3 \rho_g C_D D^2 \Delta S}{2 M_p} \right) \right] \quad (11)$$

The value of  $C_g/C_D$  is on the order of unity for conditions of significant mass loss due to ablation (Ref 7:224).

Substituting into Eqn (11) the equivalent value for the particle mass, and area in terms of particle size and density, we have after correcting for the assumed spherical fragment shape.

$$\frac{\Delta m}{m_p} = \frac{C_g V_o^2}{3 C_o (C_p T + h_f)} \left[ 1 - \exp\left(-\frac{3 \rho_f C_o \Delta S}{2 \rho_f D}\right) \right] \quad (12)$$

where  $\rho_f$  is the density of the fragment.

The left side of Equation 12 represents the fraction of the energy transferred from the kinetic energy of the particle to the surroundings. This number is in general a very small value unless  $D$  is very small,  $\rho_f$  is very small or there are a large number of particles contributing a small fraction of their energy to the system. Figure 4 represents equation 12 plotted for 10,800 ft/sec. The calculations were terminated at  $V_i = 4000$  ft/sec because that is the minimum velocity at which the stagnation temperatures are great enough to melt aluminum. Notice that with particle sizes in the 10-100 micron size the contribution is several orders higher than for the somewhat larger fragments.

Several investigators, notably Backman and Stronge (Ref 4:9) made determined efforts to collect the fragments after moderately high velocity impact events. For 1/8" thick plates and impact velocities of 3.16 and 5.7 km/sec, Backman reports that only 44% and 55% of the total mass of the projectile and target were recovered. Most of the fragments recovered were fairly large, greater than  $\sim 250 \mu$ .

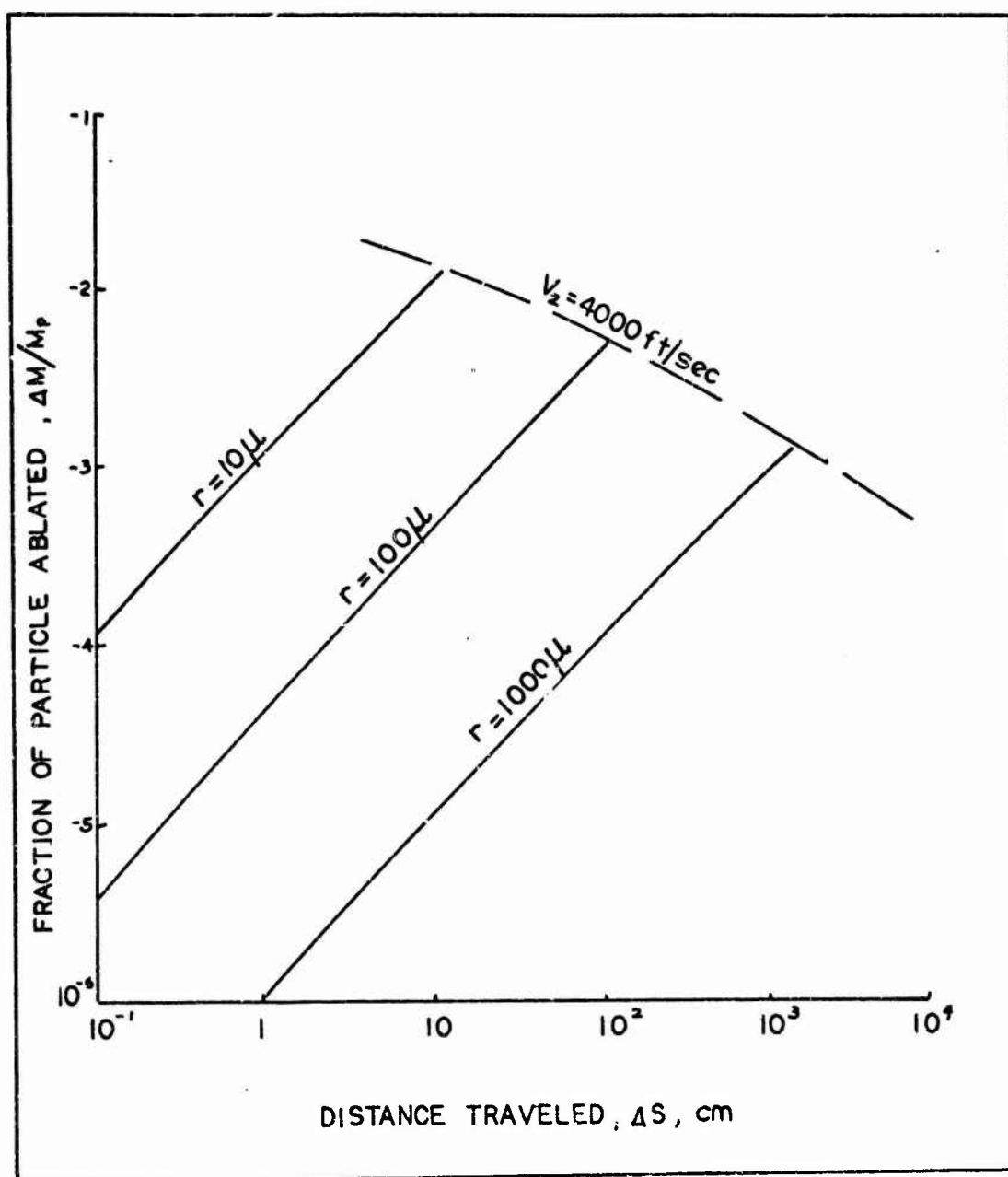


Fig 2. Ablation of Al Particle at High Velocity (10,800 ft/sec). Clearly Shows Effect of Decreasing Particle Size on Energy Deposition (Ref 4:33).

For the higher velocity impacts a considerably higher percentage of the recovered fragments were quite small, the smallest sieve size being #200 (an opening of 74  $\mu$ ).

From these data and equation 12 there exists the suggestion that there are a considerable number of very small fragments moving at very high velocity exiting the fragment hole into the box. Equation 12 also suggests an analytic confirmation of Backman's observation that the pressure build-up in the box varies with the kinetic energy of the impacting system.

What then could be the mechanism for the sometimes observed sudden pressure increase at approximately 8000 ft/sec? It is the hypothesis of this study that under certain conditions that very tiny highly energetic particles are heated aerodynamically to the ignition temperature and that extremely rapid burning occurs. The first consideration then is to show a way of predicting under what conditions these secondary particles occur. It will then be shown that the stagnation temperature at approximately the critical velocity of 8000 ft/sec in air is such that there is significant dissociation of molecular oxygen to atomic oxygen. Also at that velocity the stagnation temperature is at or above the melting temperature of aluminum oxide ( $Al_2O_3$ ) allowing rapid reaction of the energetic oxidizer and aluminum.

#### Heyda Plug-Shattering Model

A likely source of energetic micro-sized particles has

been hypothesized by Heyda (Ref 9:142). The model predicts that under certain conditions the plug driven out of a plate, subjected to high velocity impact by a flat-faced cylindrical projectile, will shatter at or near the center. For the few cases where verification was attempted, the impact velocity of incipient plug-shattering was accurately predicted. The basic development of the model is given with reference to figure 3.

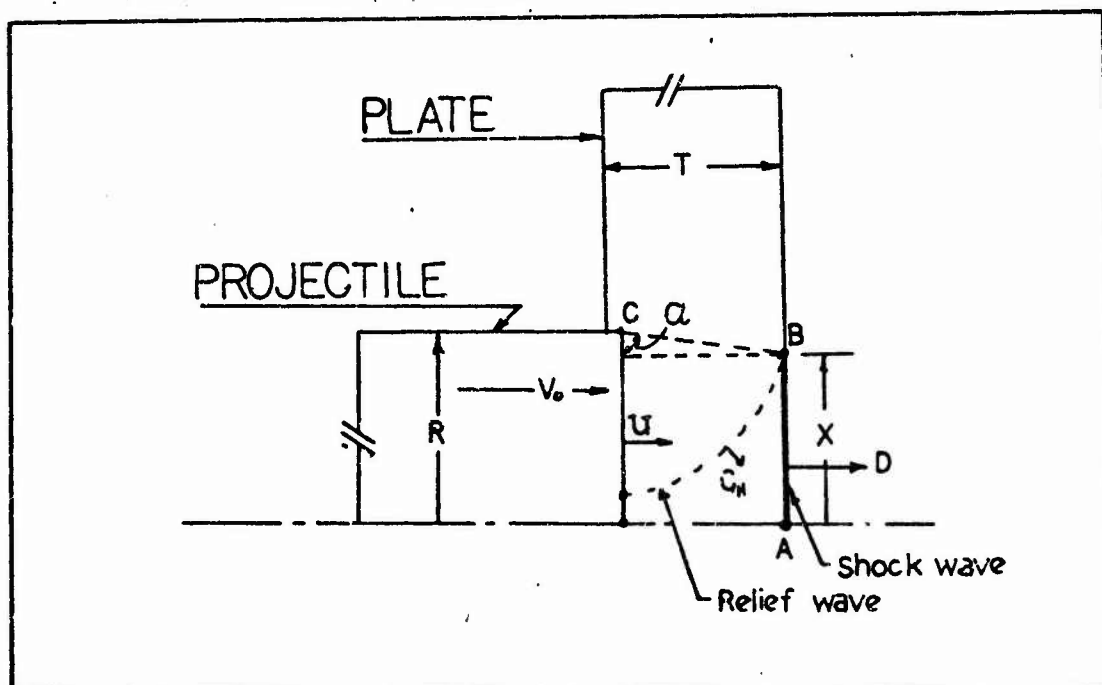


Fig 3. Geometry and Nomenclature for Development of Heyda Plug-Shattering Model (Ref 9:143).

At time  $t$ , the projectile plate interface has moved with velocity  $U$ , the particle velocity in the plate, a short distance into the plate with thickness  $T$ . Figure 3 represents the conditions at  $t$ , the instant that the planar shock front traveling at velocity  $D$  just reaches the rear surface

of the plate. The compressed region behind the shock wave is being attenuated by a relief wave emanating from the corner of the projectile at C. This relief wave moves at the hydrodynamic sound velocity  $C_u$  for the conditions behind the shock. Observe that the center of the rarefaction wave is moving at the particle velocity behind the shock  $u$ . At the instant the shock reaches the rear surface, the relief wave has started to relieve the intense pressure at B. Denoting the radius of the unattenuated shock AB as  $X$ , then at time  $t_r$  the following hold.

$$D - u = C_u \sin \alpha \quad (13)$$

$$R - X = (C_u \cos \alpha) t_r \quad (14)$$

$$T = D t_r \quad (15)$$

combining these equations

$$\left( \frac{D-u}{C_u} \right)^2 + \left[ \frac{(R-X)D}{C_u T} \right]^2 = 1 \quad (16)$$

and after considerable algebraic manipulation

$$X = R \left[ 1 - \frac{T/R}{S} \right] \quad (17)$$

where

$$S = \frac{D}{\sqrt{C_u^2 - (D-u)^2}} \quad (18)$$

Note that parameter  $S$  is a dimensionless function only of the material properties and the Hugoniot conditions which are specified by the initial velocity.

Referring to Figure 3 and equation 17 observe that if,

$$S > \frac{T}{R} \Rightarrow X > 0 \quad (19)$$

and the shock wave will not be attenuated on the axis of symmetry before reaching the rear surface of the plate. A reflection of the compression wave will occur at the air-metal interface and the familiar spallation phenomenon may occur if the reflected tensile wave is of sufficient strength and shape.

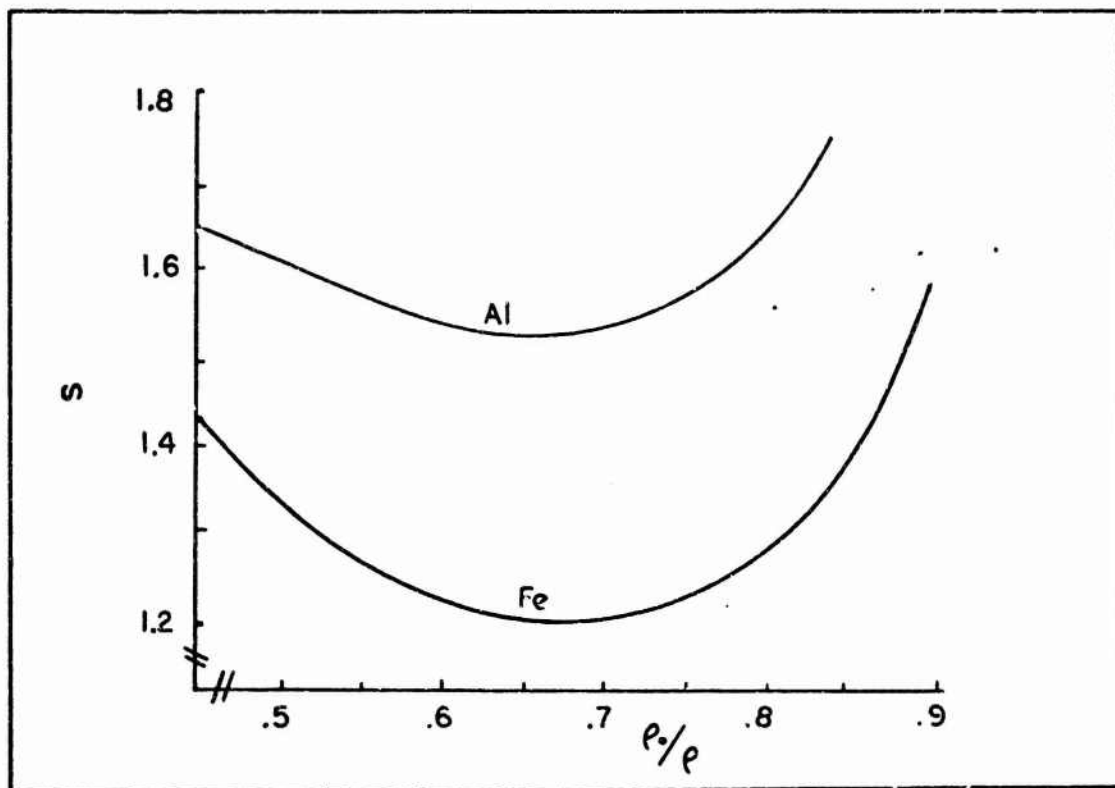


Fig 4. Plot of Dimensionless Variable  $S$  Versus the Ratio of Material Density Before Impact to Density After Impact (Ref 9:144). Additional Plots for a Wide Variety of Materials are Shown in Appendix B.

Now, consider again Figure 3 and equation 17.

If

$$S < \frac{T}{R} \Rightarrow X < 0 \quad (20)$$

which implies that the shock wave will be attenuated on the axis of symmetry before reaching the rear free surface.

"Such an attenuation point corresponds physically to the rapid deposition of energy on the axis of penetration at the point which is  $T - RS$  units from the rear surface. This rapid energy deposition approximates explosive behavior and results in plug-shattering." (Ref 8:143)

From equation 19 and 20 one concludes that there exists a critical velocity  $\bar{V}_0$ , at or above which, plug-shattering is expected to occur. The critical case occurs when

$$S = \frac{T}{R} \quad (21)$$

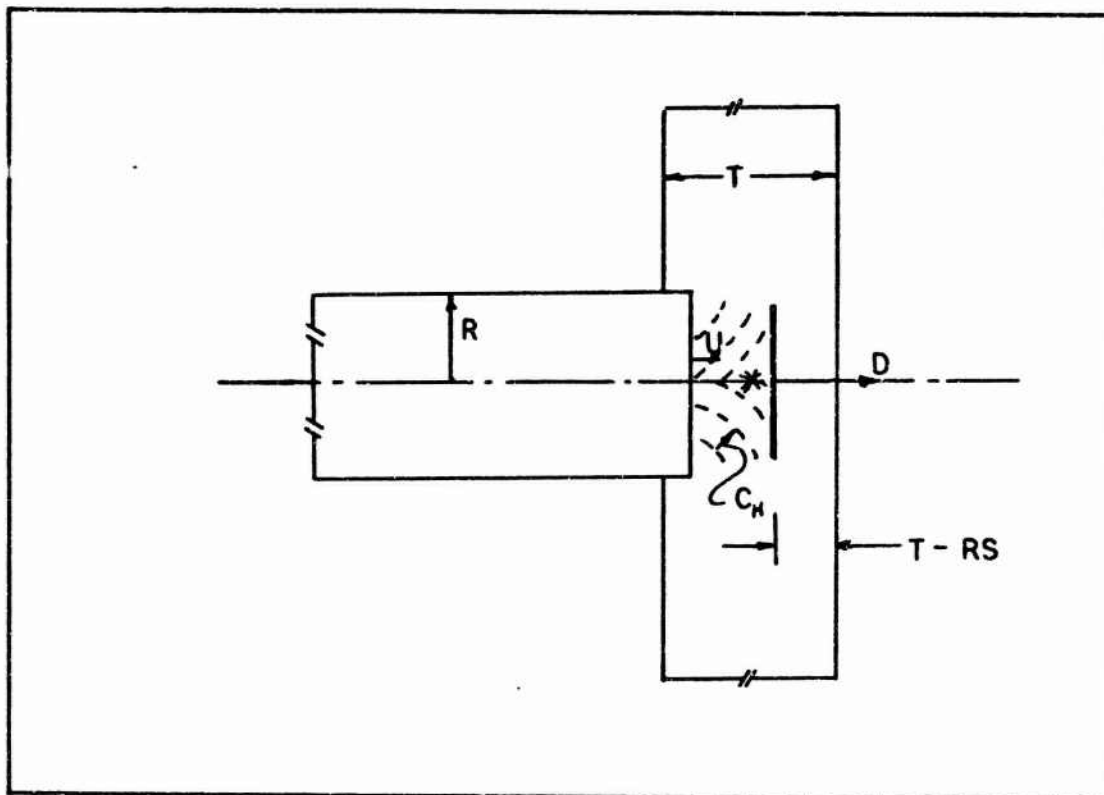


Fig 5. Case Where  $S < \frac{T}{R}$ . Energy is Deposited at Plug Centerline at an Explosive Rate.

To calculate the critical velocity  $\bar{V}_0$  at which incipient plug-shattering occurs begin with the Hugoniot continuity equation across a shock wave

$$\rho_0 D = \rho (D - u) \quad (22)$$

where  $\rho_0$  is the ambient material density,  $\rho$  is the density of the material immediately behind the shock,  $D$  is the shock front velocity and  $u$  is the particle velocity in the material behind the shock.

Combining equation 22 with the well known empirical relation

$$D = A + Bu \quad (23)$$

where A and B are empirical constants the values of which are summarized in AFWL-TR-69-38 (Ref 9), one gets

$$u = \frac{A}{\left(\frac{1}{1-\rho/\rho_p}\right) - B} \quad (24)$$

for the particle velocity in the plate.

In the projectile, equation 23 becomes

$$\bar{D} = \bar{A} + \bar{B} (V_0 - u) \quad (25)$$

where the superscript bar implies properties of the projectile.

Finally, after considerable manipulation, it can be shown (Ref 8:145) that the critical velocity for incipient plug-shattering is given by

$$\bar{V}_0 = u + \frac{1}{2\bar{B}} \left[ \sqrt{\bar{A}^2 + \frac{4\bar{B}\rho_p}{\bar{\rho}_p} u(A + B u)} - \bar{A} \right] \quad (26)$$

where  $\bar{\rho}_p$  is the density of the projectile prior to impact.

Experimental data contained in Woodall (Ref 8:146) shows for a steel cylinder of radius 0.391 in impacting a steel plate of thickness 0.635 in at a velocity of .777 km/sec (2550 ft/sec) showed signs of shattering type failure at the plug's axis of symmetry. A calculation of the expected critical velocity, the velocity at which incipient plug-shattering would occur, indicates  $\bar{V}_0$  should be 2619 ft/sec. This suggests excellent agreement between experiment and a simple model. The details of the calculation are shown in Appendix A.

Extrapolation of the Heyda Plug-Shattering Model to Spherical Projectiles

Above we have seen that the Heyda plug-shattering model predicted fairly well when incipient shattering will occur for a flat-faced cylindrical projectile impacting a plane plate. Since it is stated by Swift (Ref 10:518) that little is known quantitatively about the material shattering processes, it may be appropriate to make a heroic extension of Heyda's model to other shapes.

Heyda's derivation assumes a planar shock is generated by the plane face of the cylinder which creates a region of very high pressure in a region behind the shock which is then relieved by a rarefaction wave converging on the axis of symmetry with explosive results.

Consider a sphere impacting a plate. At the point of impact at the instant of impact there will be some deformation of the projectile and plate which would approximate a planar impact of a smaller cylinder. Note that Heyda's model depends only on material properties, impact velocity and geometry of the impact, there is no restrictions on the mass (or length) of the projectile.

To make such an extension of Heyda's model one would, of course, prefer to predict on sound theoretical grounds which parameters would or could equate different shapes. In this extension for example, an equivalent radius  $R^*$  is proposed which equates a spherical contact surface to a plane

circular surface. It appears to be a formidable, if not impossible, task to find such a theoretical relation. A second choice would be to use one of the very complex (and time consuming) computer hydrodynamic codes such as CRAM, PICKWICK, VISTA OR HELP (Ref 11:163). An objective of this study was to minimize complex calculations for the first order analysis so the computer codes were not extended to include this problem. The final alternative was to look at the very limited experimental data which reported information from which one might attempt an extension. The best source of these data are reported in Hopkins, Lee and Swift (Ref 12).

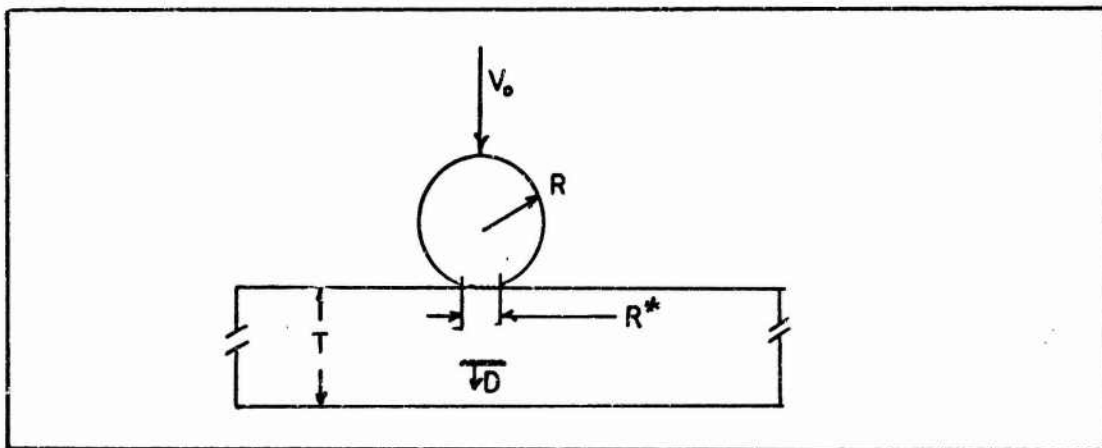


Fig 6. Geometry of Spherical Projectile Impacting a Plate for Extension of Heyda Plug-Shattering Model.

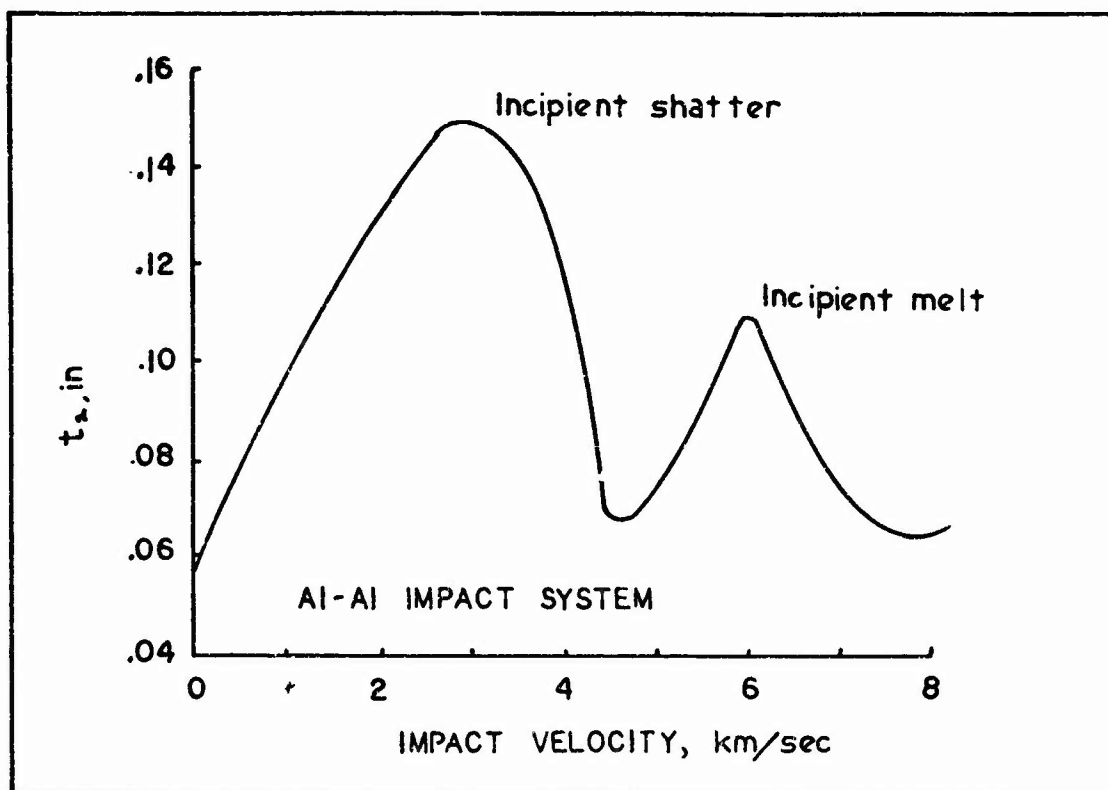


Fig 7. Ballistic Limit Curves;  $t_w$  is Thickness of Witness Plate (Ref 12)

Before describing the method for estimating  $R^*$ , the equivalent radius for a sphere which allows one to use Heyda's model, an explanation of the source of empirical data is required. Hopkins, Lee and Swift were attempting to learn more of the role of shock heating in determining the performance of two element hypervelocity impact shields. A series of tests were run where an aluminum projectile of 3.17 mm diameter was propelled through an aluminum bumper plate 0.787 mm thick. The thickness of the hull plate consisting of 6061-T6 aluminum was varied until a ballistic limit was found for a given impact velocity. Figure 7 shows the thickness of the hull plate at the ballistic limit  $t_w$  for

a wide range of impact velocities. At the point indicated as "incipient shattering" some part of the system is presumed to shatter into smaller pieces, assumed to be the plug in accordance with the Heyda model.

Using 3.0 km/sec taken from Figure 7 equations 24 and 22 were solved in reverse for  $\frac{P_0}{\rho}$ . Using figure 4, or charts shown in Appendix B, a corresponding S was found. Since at the critical velocity  $S = \frac{T}{R}$  and T was fixed, an equivalent  $R^*$  was found. The ratio  $R^*/R$  was found to be between .25 and .30 for all experimental evidence of incipient plug-shattering found. The details of one calculation are shown in Appendix A.

In summary, an argument has been presented which implies that a source of energy which causes a pressure increase in a closed box is dependent on numerous, very tiny, rapidly moving secondary fragments. One source of these fragments under certain circumstances of velocity, plate thickness and impact particle size and density would be the explosive release of energy in the center of the plug as predicted by the Heyda model. Presumably these fragments would have a velocity greater than that which would be expected from a like-material impact, with spallation. For a spallation event the secondary fragments have an initial velocity of twice the plate particle velocity which is, for like-material impact, one-half the initial impact velocity. Or more concisely, for like-material spallation event the secondary

fragments will have the same velocity as the impacting projectile.

It is also true that there will be other small fragments of somewhat lower velocity than either the plug, the impacting projectile, the traditional spallation fragments or the shattered plug fragments (if the conditions exist). These small fragments at a lower velocity are associated with the buildup of a combination of tensile and shear stresses in the plate induced by the wedging interaction between the projectile and target as the projectile passes through (Ref 8:377).

There is, therefore, a wide distribution of velocities for the secondary fragments possible. It would be difficult if not impossible to specify an exact distribution for all cases. For the purpose of further analysis micro-sized fragments will be assumed to come from the plug-shattering event. Further, the assumption will be made that at least some of these fragments will have, as a minimum, the velocity of a spallation fragment, 8000 ft/sec. Complex computer codes may be modified to give a more accurate estimate.

The next step is to consider what effect these fragments may have on the pressure build-up in a box.

#### Aerothermodynamic Effects on Secondary Fragments

Having considered a source of high velocity secondary fragments and focusing attention on the very small fragments,

in the tens of micron size and a velocity of 8000 ft/sec, the next step is to consider the aerothermodynamic effects on these fragments and their immediate surroundings. It is the hypothesis of this study that these fragments will burn almost immediately at or above the critical velocity being considered. In simplest terms the requirements for burning are: (1) a fuel, a material that will react rapidly with oxygen (or other element) exothermally; (2), an oxidizer, oxygen, in the form of atomic oxygen, O, not O<sub>2</sub> or the oxygen ion O<sup>+</sup>; and, (3) a source of heat which will raise the temperature of the system to the ignition temperature.

Fragment Heating. Before making claims as to the amount of heating of the air it is necessary to know if the flow field can be treated as a continuum, in which the commonly used hypersonic analysis have been performed. The usually accepted criteria for continuum flow is the Knudsen number,  $K_n$ , which is the ratio of the molecular mean free path,  $\lambda$ , to some characteristic dimension of the flow field  $L$ . If  $K_n$  is very much less than unity then the flow is a continuum (Ref 13:210). At sea level for a 50 micron fragment,

$$K_n = \frac{\lambda}{L} = \frac{30 \times 10^{-9} \text{ M}}{50 \times 10^{-6} \text{ M}} = 6 \times 10^{-4} \ll 1 \quad (27)$$

Therefore, the classical continuum analysis will be used for a real gas.

The first consideration is the temperature of the air surrounding the fragments. Figure 8 shows the temperature

immediately behind a hypersonic shock wave of a cylindrical fragment moving in air at sea level and 35,000 ft. Note that at 8,000 ft/sec the temperature is approximately 2790 K if the initial temperature was 300 K. The boiling temperature of Al is 2350 K (Ref 15).

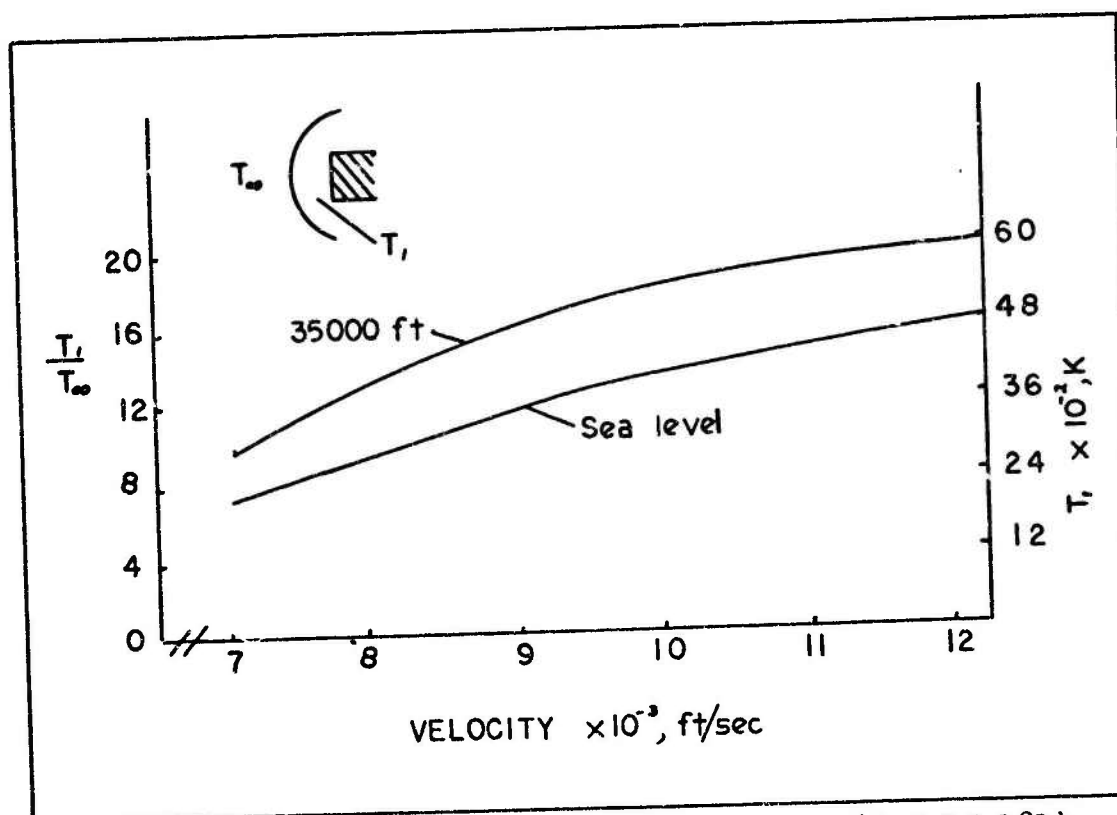


Fig 8. Temperature Behind Hypersonic Shock (Ref 15:181)

Figure 9 represents the temperature at the stagnation point on a cylindrical fragment. At 8000 ft/sec the temperature is approximately 2730 K. It is well known that the ignition temperature for aluminum is approximately 2300 K (Ref 16) which is below the ambient temperature of a particle with a velocity of 8000 ft/sec.

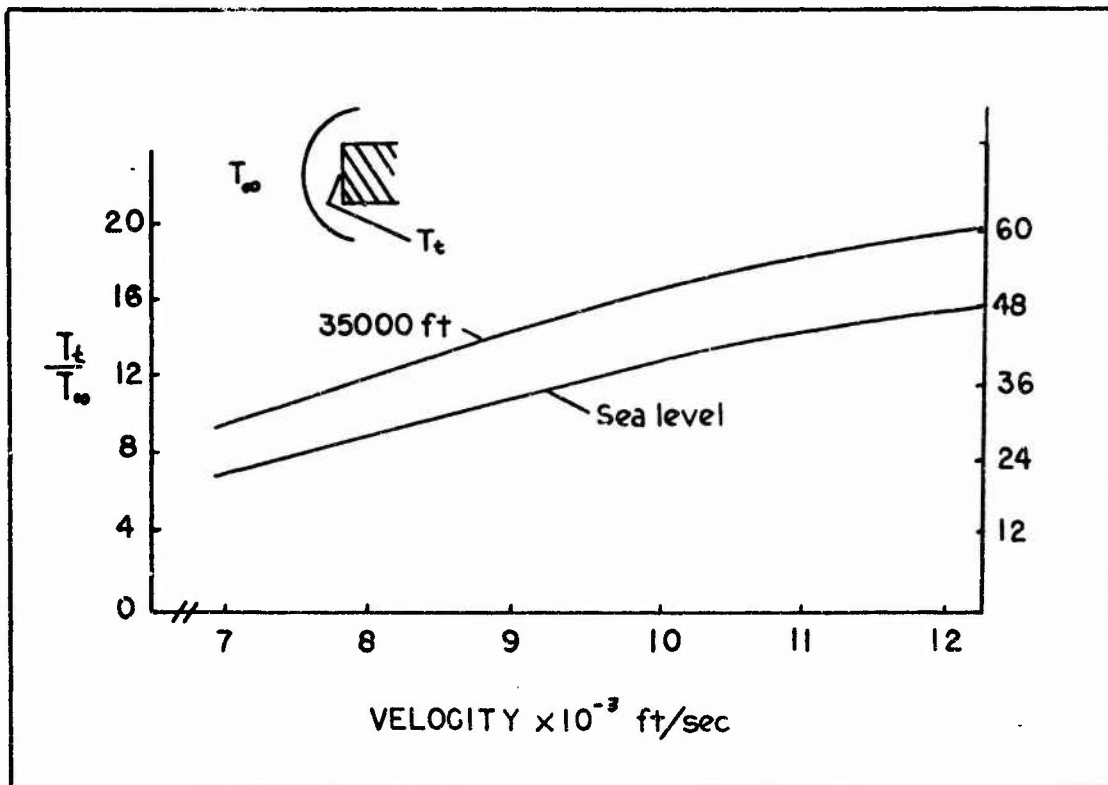


Fig 9. Stagnation Temperature for a Circular Cylinder  
(Ref 15:183)

One would then be concerned why all aluminum projectiles do not burn up entirely when traveling at velocities in the neighborhood of 8000 ft/sec. Fay & Riddell (Ref 13:183) point out that the heat transfer rate to the body  $q_b$  is a function of the air density  $\rho$ , and the radius of the entry face of the projectile  $r_b$ . Figure 10 represents the relationship between these parameters and the free stream velocity.  $T_w$  is the temperature of the body. Note particularly that for very tiny fragments, micron size, that the heat transfer rate to the body is extremely high, in fact the smaller the fragment the faster it will heat to the ignition temperature and supply the necessary heat required

for any energy threshold which might exist which would delay ignition. The key point on Fig 10, however, is that at approximately 8000 ft/sec for a very hot body, the heat transfer rate achieves a positive value. Ignition will occur only if enough energy is added to the system to heat a slab of aluminum on the fragment as thick as a steadily propagating adiabatic laminar flame to the ignition temperature (Ref 16:188).

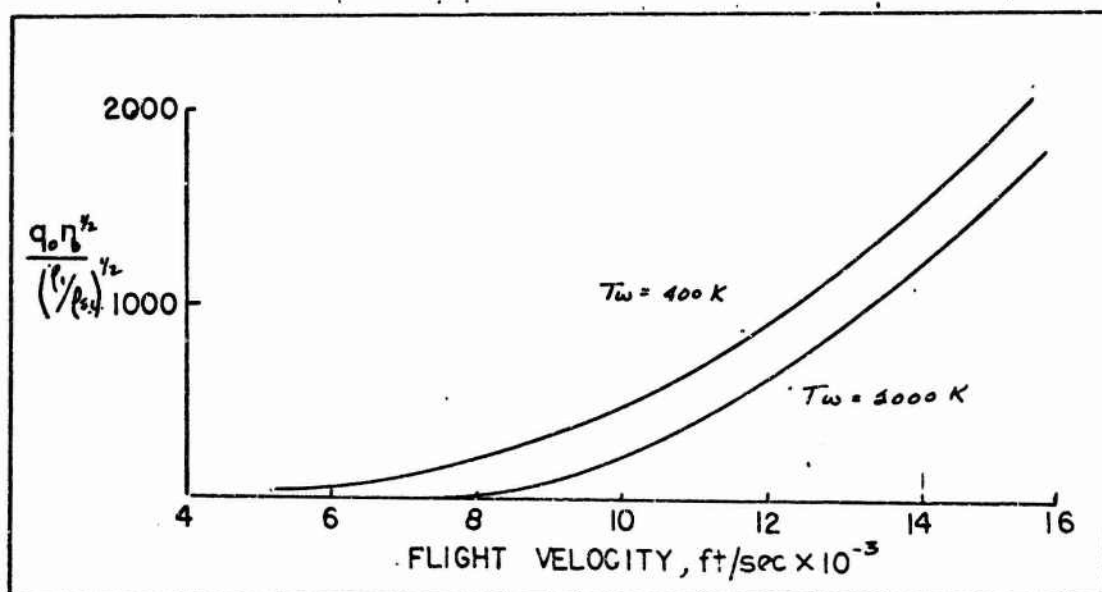


Fig 10. Stagnation Point Heat Transfer in Laminar Equilibrium Dissociated Flow (Ref 13:184)

#### Effects on Ambient Atmosphere Surrounding Fragments.

At 8000 ft/sec the secondary fragments are exposed to temperatures of approximately 2700 K or 400 K greater than the ignition temperature of aluminum. This section will address the concentration of high temperature oxidizer surrounding the fragments.

For a real gas the pressure of the gas in the neighborhood of the fragment is important. Figure 11 and 12 show the pressure behind the shock wave and at the stagnation point for a cylindrical fragment as a function of velocity. It is interesting to note that, at least for a part of the environment, the pressure acting on the surface of fragment is approximately 50 atmospheres.

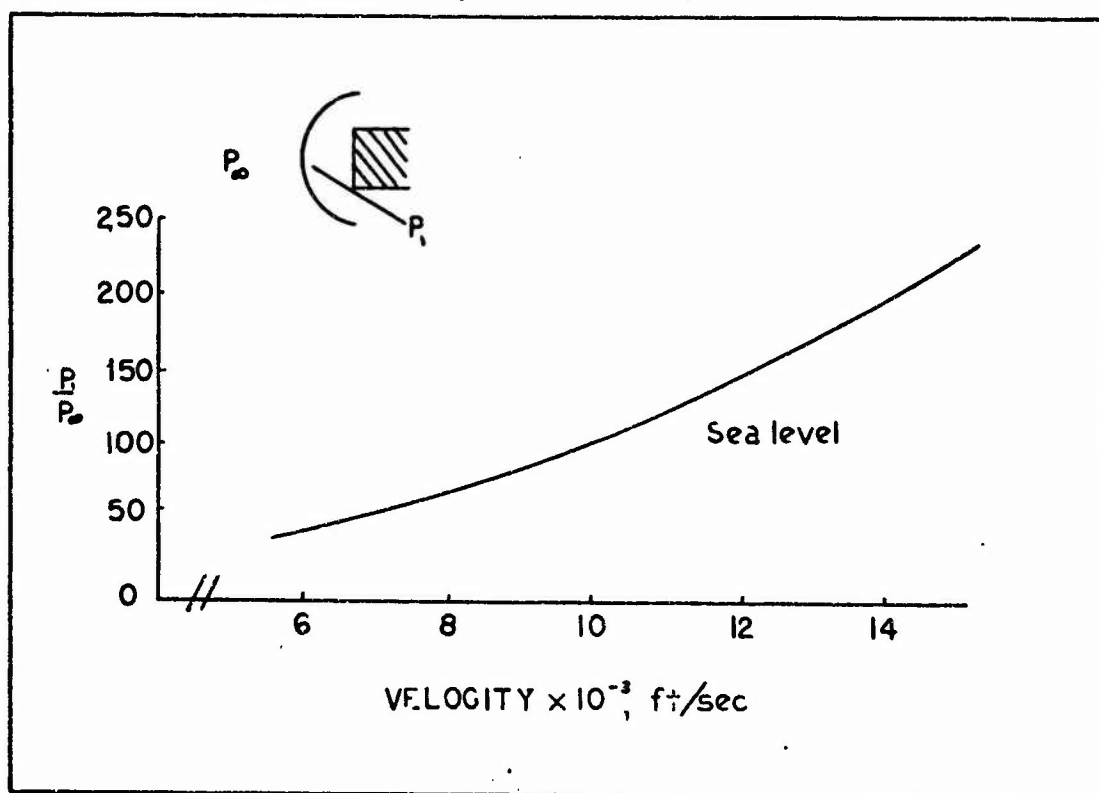


Fig 11. Pressure Increase Across Shock Wave for a  $P_0$  at Cylindrical Body at Hypersonic Velocities (Ref 15:172)

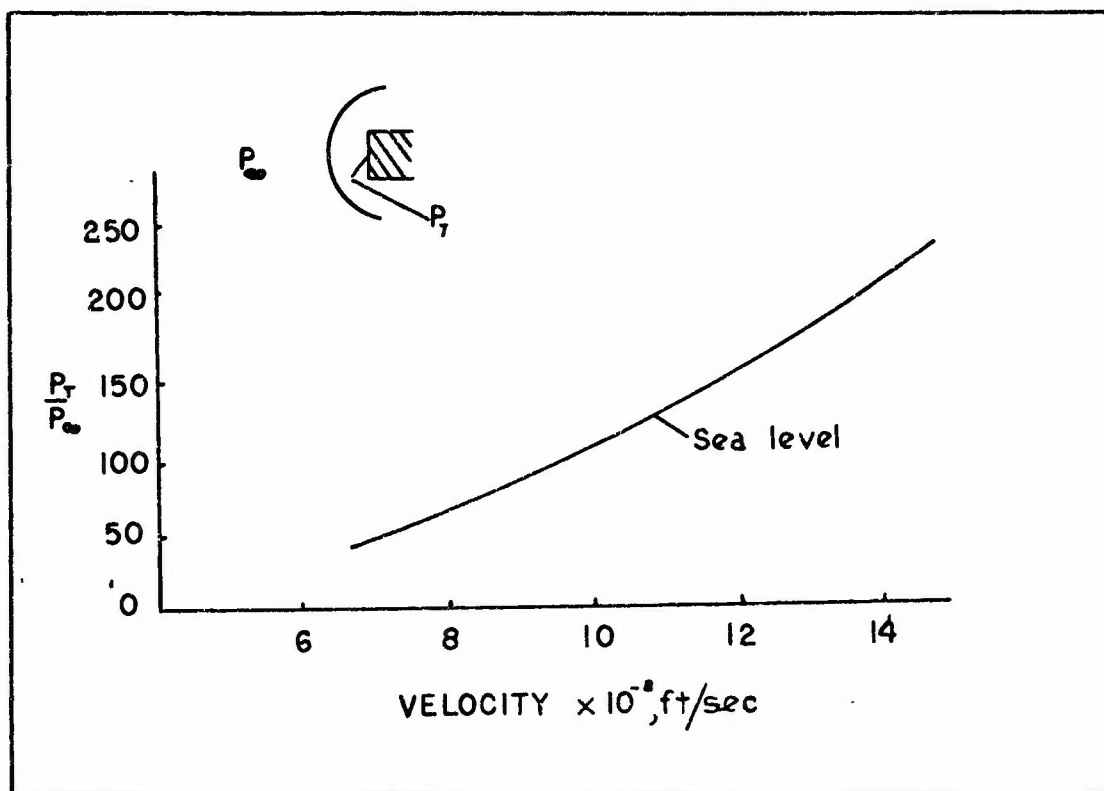


Fig 12. Stagnation Pressure at Leading Edge of a Right Cylinder at Hypersonic Velocities (Ref 15:178)

Another consideration is the chemical effects on air at these very high velocities. Figure 13 suggests a very important consideration, coincidental with 8000 ft/sec flow. At that velocity dissociation of molecular oxygen into atomic oxygen becomes significant.

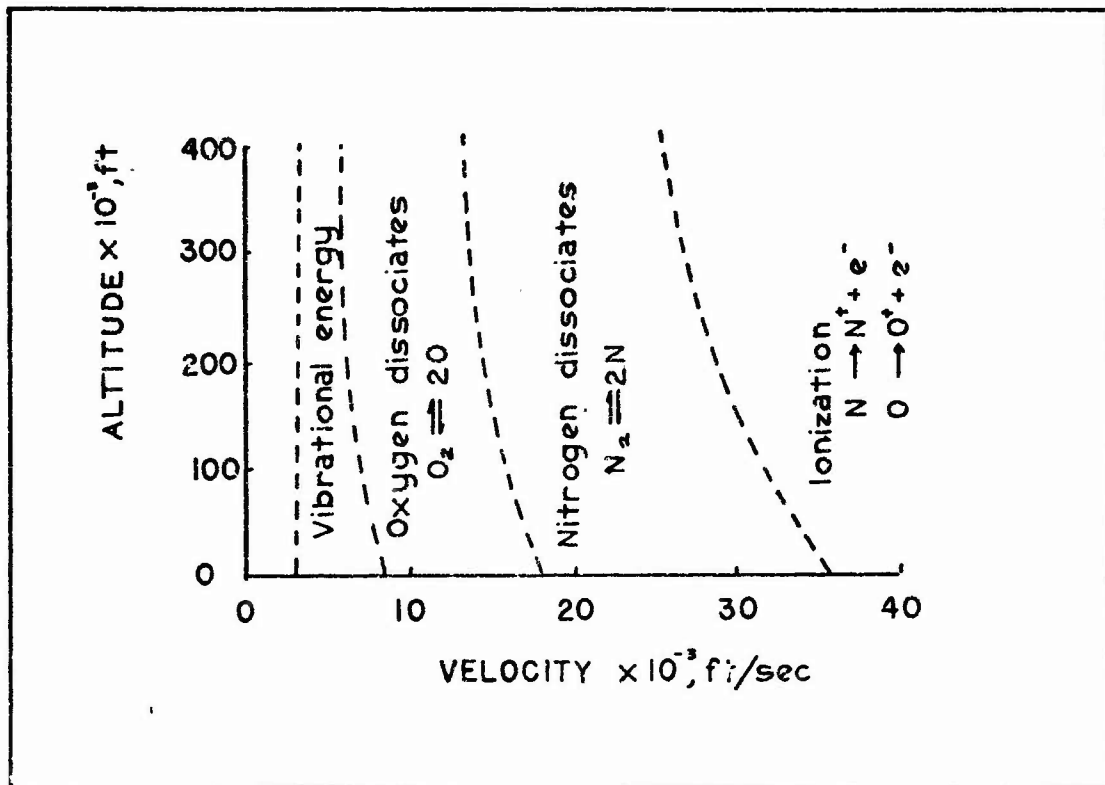


Fig 13. Chemical Effects of Air at Various Velocities and Altitudes (Ref 17:21)

Another representation of similar data, taken from Cox and Crabtree (Ref 13:161) relates the compressibility factor,  $Z$  which is defined by

$$Z = \frac{P}{m \rho R T} \quad (28)$$

where  $P$  is the gas pressure  
 $\rho$  is the gas density  
 $R$  is the universal gas constant  
 $T$  is the absolute temperature of the gas  
 $m$  is the molecular weight of the gas

in consistent units. The parameter  $Z$  can be represented by  $1 + \alpha$ , where  $\alpha$  is the fraction of initial moles of gas

which has dissociated (Ref 3:108) and therefore represents a deviation from ideal gas law. The greater the value of  $\alpha$  the more the gas deviates from an ideal gas. From Fig 14 note that just above a temperature of 2500 K the dissociation of molecular oxygen begins to change the behavior of a gas. This deviation from ideal gas behavior has been implicit in all arguments presented in this section.

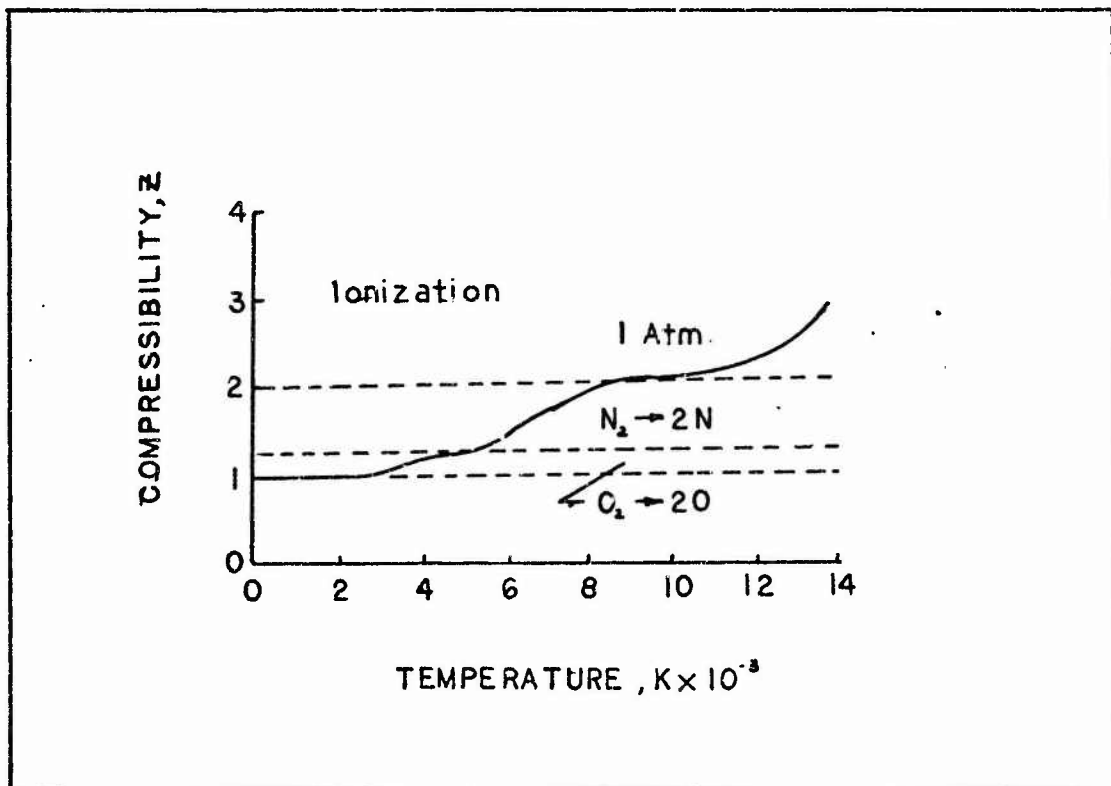


Fig 14. Compressibility Factor for Air (Ref 18:123)

Combustion and Ignition of Aluminum Fragments. In the past two subsections it was shown that if fine particles of aluminum are traveling through air at approximately 8000 ft/sec that the aerothermodynamic heating will, coincidentally,

cause temperatures surrounding the particle to rise to the ignition temperature, and that the smaller the fragment the greater the heat transfer to the fragment. Additionally, at that critical velocity air begins to dissociate to atomic oxygen, an extremely powerful agent for supporting burning of aluminum, or any other combustible material. The next subject will address briefly some of the phenomena necessary for an aluminum particle to burn almost instantaneously, in the environment that exists around the fragment while moving at approximately 8000 ft/sec.

Friedman and Macek (Ref 18:15) in their theoretical and experimental investigation of the burning of aluminum particles conclude that the melting point of alumina ( $\text{Al}_2\text{O}_3$ ),  $2300 \pm 20$  K, is very important for ignition of aluminum. At that temperature the alumina melts which allows the diffusion of the oxygen to the aluminum. They point out that theory predicts that the ignition should depend strongly on the concentration of oxygen, but as is shown by Fig 15, the ignition limit is relatively insensitive to the concentration of oxygen.

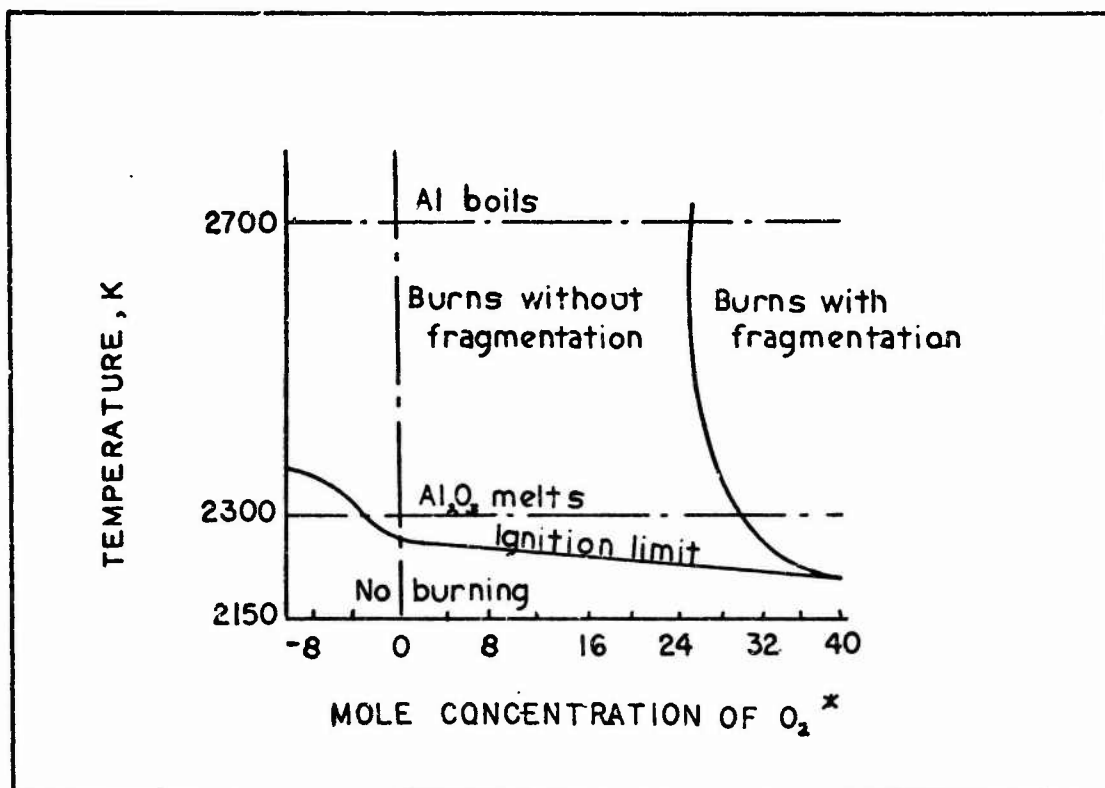


Fig 15. Experimental Ignition and Fragmentation Limits  
 (35  $\mu$  Diameter Aluminum) (Ref 18)  
 \* Minus Concentration Implies Deficiency From Stoichiometric Concentration.

The key to combustion and combustion rates at elevated temperature then seems to be that a reaction will begin where the oxide coating surrounding the at least partially molten fragment can be penetrated by oxygen or as in the case of the high velocity environment, atomic oxygen. Almost instantly, the temperature rises to greater than 2350 K, the boiling point of aluminum, and the reaction takes place in a gaseous system. For observed cases an increase in pressure is recorded approximately 50  $\mu$  sec after impact (Ref 4:46-54) so the ignition time is of utmost importance, if burning is to be considered an important contribution to the sudden

pressure increase. Delayed ignition could also contribute significantly by increasing the duration of the unaugmented pressure pulse associated only with a high velocity impact.

Belyaev (Ref 19:323) measured the ignition time and burning time of aluminum particles in high pressure oxidizing atmosphere. The pressure range covered was 10-100 atmospheres which was shown in Fig 11 and 12 to be the applicable case for 8000 ft/sec flow. Their results show that for a  $70\mu$  diameter fragment the ignition time is essentially zero for temperatures above 2500 K. Fig 16 illustrates their data.

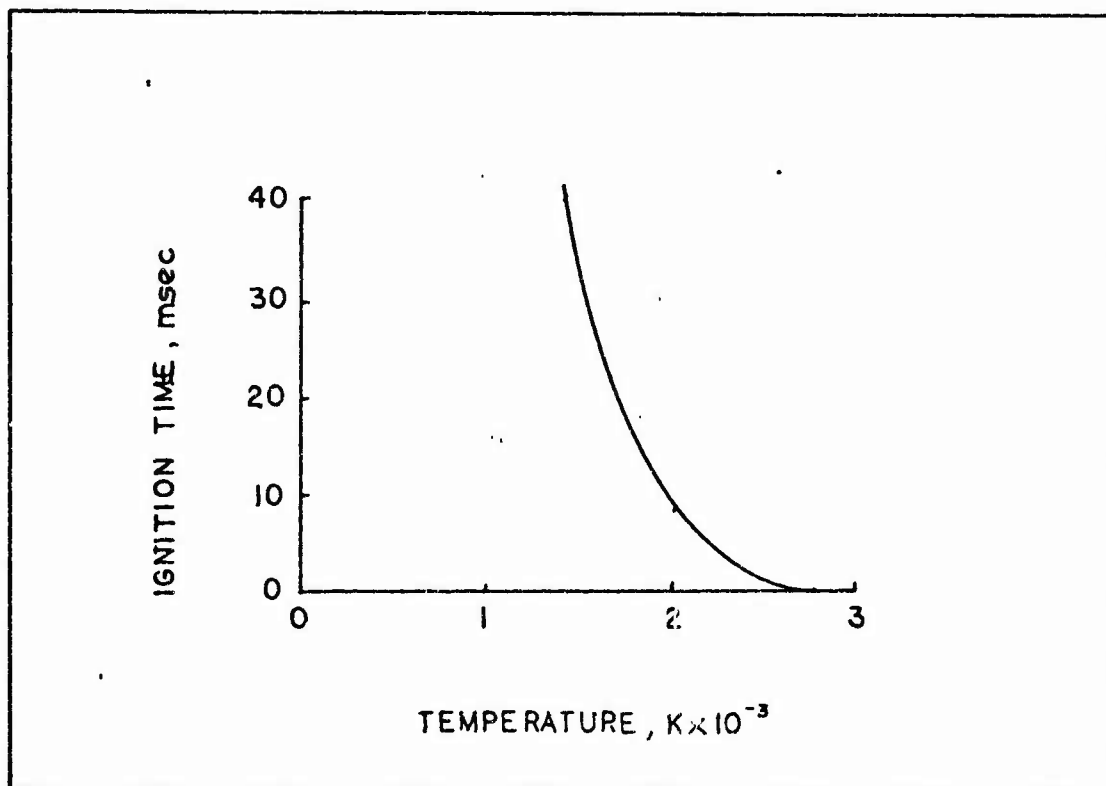


Fig 16. Ignition Time for  $70\mu$  Al Particles in High Temperature Air (Ref 19:324)

They also show that the burning time is a strong function of the particle diameter and the strength of oxidizer which they characterize by the parameter  $a_k^r$ . They did not consider the effect of atomic oxygen in the reaction.  $a_k^r$  represents the activity of the oxidizer and the concentration, a higher value implies a more energetic reaction. An assumption must be made that a high concentration of atomic O would be a more energetic atmosphere than an atmosphere where the oxygen carriers are CO, H<sub>2</sub>O, or CO<sub>2</sub> as was the case in which their experiments were carried out.

The amount of energy released by burning fragments must, therefore, depend on the burning time. Figure 17 shows Belyaev's data for burning time of aluminum.

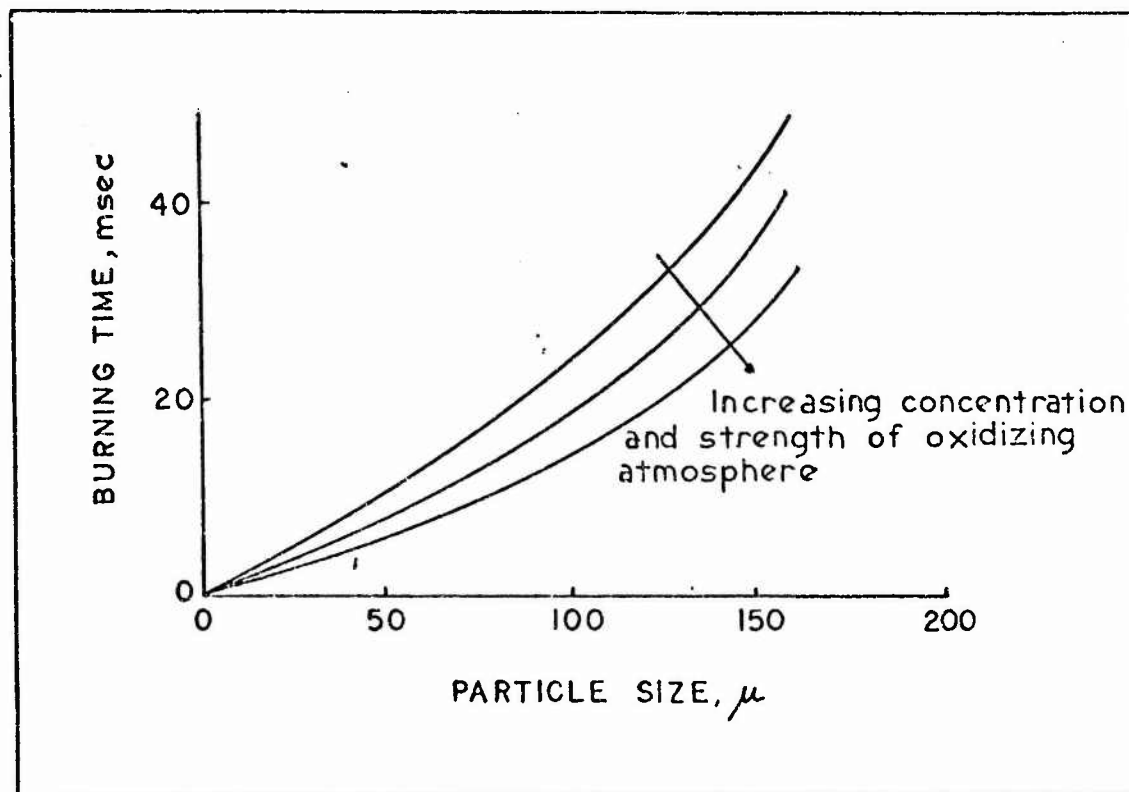


Fig 17. Burning Time of Al Fragments as Function of Particle Size and Activity of Oxidizing Atmosphere (Ref 20: 323)

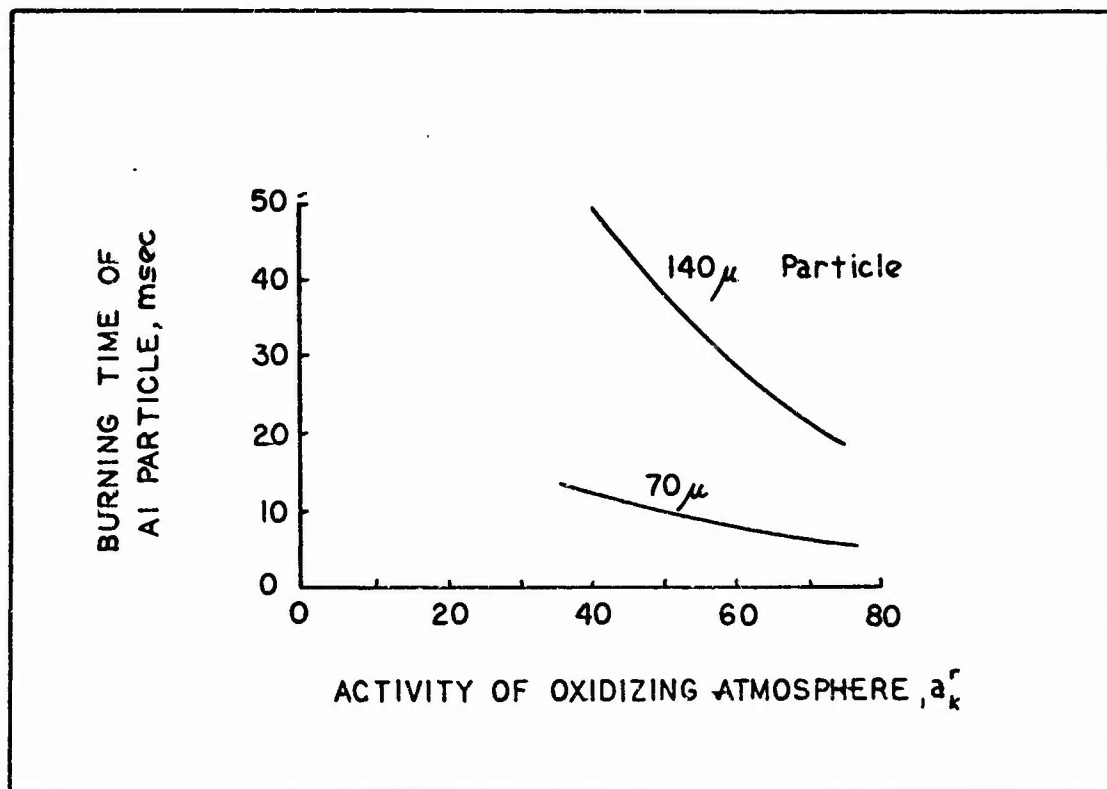


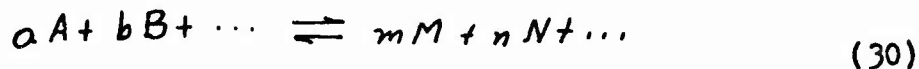
Fig 18. Burning Time of Al Particles as Function of Activity.  $a_k^r$  Represents Concentration and Availability of Free Oxygen, Increasing  $a_k^r$  Implies Greater Activity. (Ref 20:323)

From Fig 17 and 19 it is clear that the rate of energy release is a strong function of the oxidizing capability of the atmosphere and the size of the fragments. As was mentioned above, at approximately 8000 ft/sec the temperatures surrounding the fragment are approximately 2500 K and that air begins to deviate from ideal gas behavior because of dissociation of  $O_2$  to atomic oxygen.

A parameter which will indicate the amount of O in the surroundings is the equilibrium constant  $K_p$ .  $K_p$ , based on partial pressures, is defined by

$$K_p = \frac{p_M^m p_N^n \dots}{p_A^a p_B^b \dots} \quad (29)$$

where for any general chemical reaction between gases



$a, b, \dots, m, n, \dots$  represent stoichiometric coefficients for the species  $A, B, \dots, M, N, \dots$ .

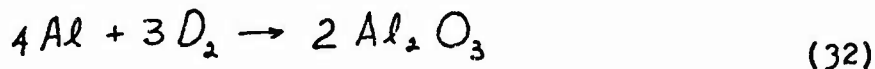
$K_p$  is related to the standard free energy change  $\Delta F^\circ$ , by

$$\Delta F^\circ = -RT \ln K_p \quad (31)$$

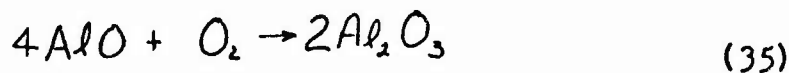
where  $R$  is the gas constant and  $T$  is the absolute temperature.

The standard free energy of formation of  $Al_2O_3$  at the ignition temperature, 2300 K, is -148 Kcal per mole (Ref 14), a very negative value implying a very strong affinity of the metal for oxygen. In fact, the reaction will proceed at a partial pressure of  $10^{-14}$  atmospheres of molecular oxygen.

The kinetics of the chemical reaction



are not well known. But there is reason to believe that at the temperatures associated with the diffusion flame of burning Al that the reactions



all proceed (Ref 3:58) which suggests a chain reaction in which the presence of atomic oxygen as a chain carrier significantly speeds the rate of reaction (Ref 16:366). Spectrographic analyses of the impact flash show the pressure of AlO (Ref 4:38) reaches a maximum 4-180 sec after the ballistic shock. As a point of interest Fig 19 indicates the partial pressure of atomic oxygen as a function of velocity. Note that at 8000 ft/sec the partial pressure of O in air is  $10^{-2}$  atmospheres.

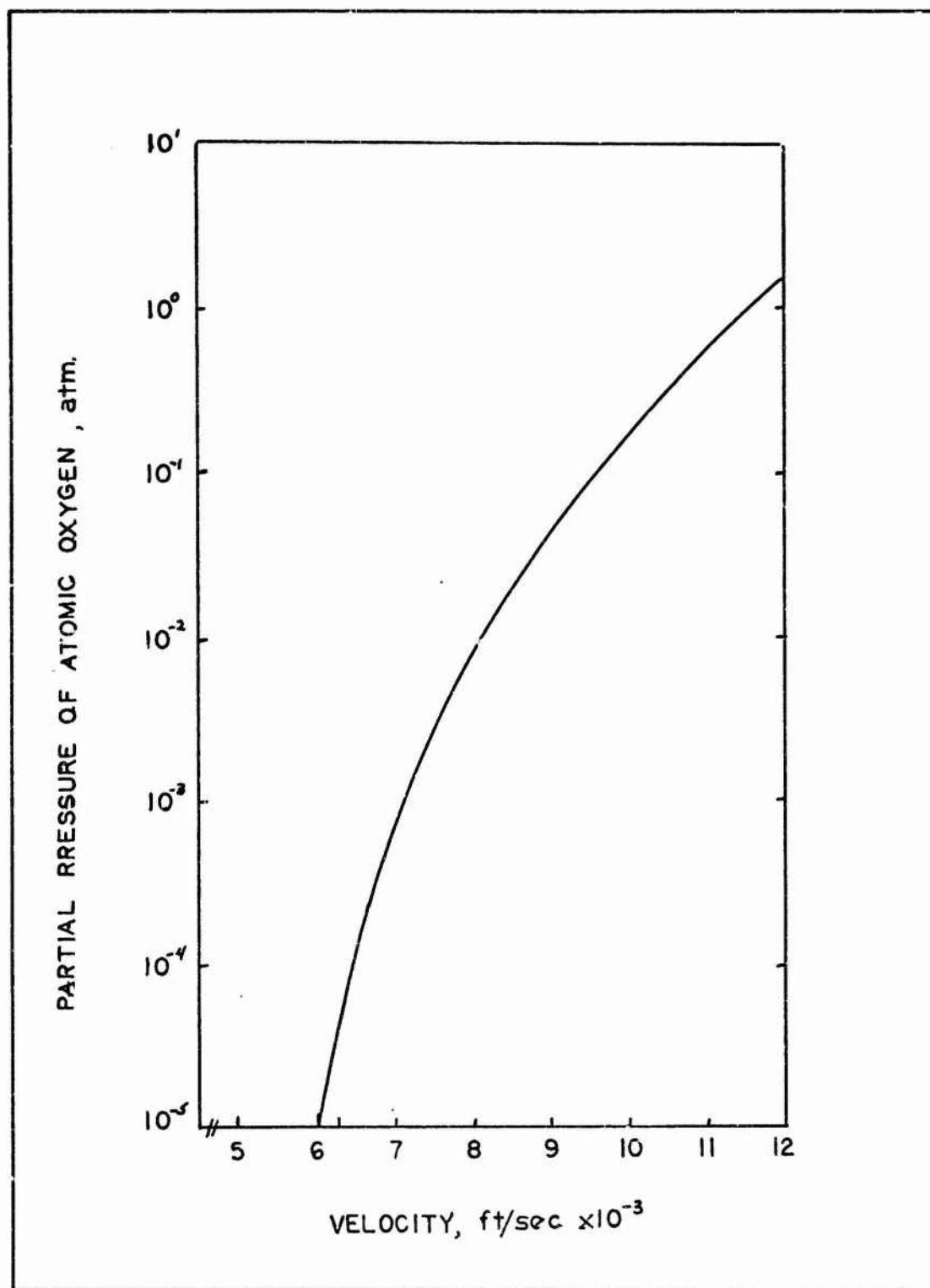


Fig 19. Partial Pressure of Atomic Oxygen as a Function of Particle Velocity, Calculated from Eqn 31 and Fig 8.

Backman (Ref 4:31) reports that by replacing air in the box with nitrogen or argon that the pressure rise is undiminished when compared to air in the box. He concludes, logically, that burning cannot occur. Assuming that he used 99% pure  $N_2$  or Ar the remaining gas being air, and approximately one-third of the plug is shattered into small enough pieces, less than  $100 \mu$  diameter, there is still twice as much  $O_2$  necessary to consume the Al fragments.

#### Summary of Damage Mechanism

In an attempt to explain the mechanism for a sudden rise in pressure in an Al box when impacted by Al fragments at or above 8000 ft/sec the following hypothesis was presented.

First, a source of high velocity secondary fragments must be found. This may occur by a mechanism as postulated in the Heyda plug-shattering model. For Al-Al systems the velocity where this occurs is in the neighborhood of 7000-12,000 ft/sec depending on geometry.

Second, at 8000 ft/sec the hypersonic conditions provide a source of heat sufficient to raise the temperature of the fragments to slightly above the ignition point of Al.

Third, at 8000 ft/sec significant dissociation of molecular oxygen to atomic oxygen takes place which provides a very energetic oxidizer to the system.

Therefore, as every volunteer fireman knows, if ignition temperatures, oxidizer and fuel are present a fire must follow.

### III. Design Considerations

Since any application of the synergistic damage mechanism would most likely involve weapons, this section will indicate some factors which would be considered in such a design. Practically, the probability of achieving enhanced damage would depend directly on creating a large number of micron size fragments moving in a closed, or nearly closed box at a velocity in the neighborhood of 8000 ft/sec or higher. The design of a weapon would revolve about creation of a large number of suitably shaped fragments. All designs do not involve only Al-Al impacts. A computer program was prepared to evaluate the plug-shattering phenomenon for a variety of materials.

#### Plug-Shattering for Other Than Al-Al Impacts

From the Heyda plug-shattering model it was concluded that when the ratio of projectile radius to plate thickness was greater than the parameter  $S$ , defined by equation 18, plug-shattering may occur. Fig 5 and the charts in Appendix B present a relationship between the parameter  $S$  and the ratio of densities before and after impact in the plate. Knowing the density ratio it is then possible to calculate the particle velocity in the plate by equation 18. Then from the material properties, specifically the empirical constants  $A$  and  $B$ , a critical velocity  $\bar{V}_0$  associated with incipient plug-

shattering may be determined from equation 26. Note that the alike material impact is not necessary for the plug-shattering event to occur.

For unlike materials, for example, a stainless steel projectile impacting an aluminum plate, the critical velocity for shattering is somewhat less than that of an aluminum projectile impacting a like plate. Fig 20 illustrates that for a given set of conditions, the stainless projectile causes shattering at considerably lower velocity.

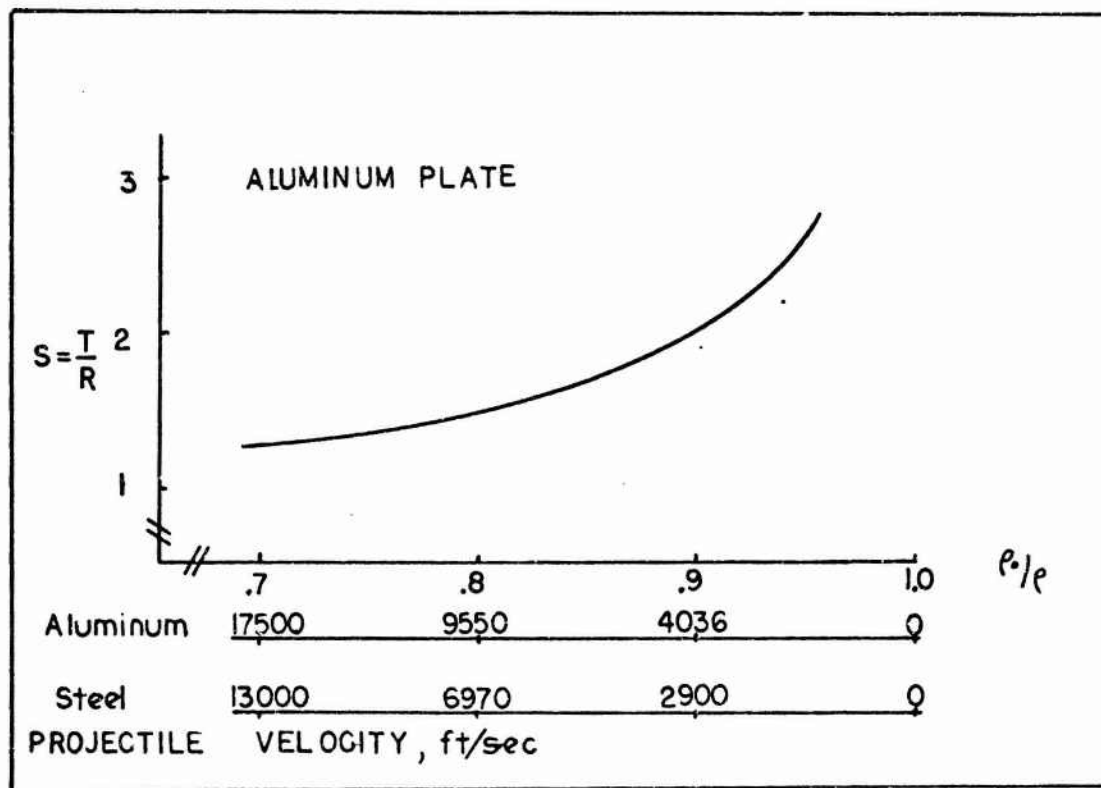


Fig 20. Velocity Required for Al and Steel Projectiles at Incipient Plug-Shattering.

If curves for a projectile-plate system are available then the calculation of a critical velocity is very straight forward. Appendix B presents curves plotting the relationship for a variety of materials which may be used for the calculation. However, if curves for the material of interest are not available the problem is somewhat more difficult.

The definition of the parameter S is given by

$$S = \frac{D}{\sqrt{C_H^2 - (D-u)^2}} \quad (18)$$

By assuming a density ration,  $\rho_p/\rho$  the particle velocity is found immediately from

$$u = \frac{A}{\frac{1}{1 - \rho_p/\rho} - B} \quad (24)$$

and the shock velocity in the plate D is then found from

$$D = A + B u \quad (23)$$

The value for the hydrodynamic sound speed  $C_H$  is not readily available or calculable from elastic theory for pressure regimes of 400 kilobars. Fortunately, AFWL-TR-69-38, Compilation of Hugoniot Equations of State, contains an empirical equation of state for a wide variety of materials. (It also contains values for A and B and the density.)

Recall, that the definition of the sound speed is given by

$$C_H = \sqrt{\left(\frac{\partial P}{\partial \rho}\right)_s} \quad (36)$$

for an isentropic wave.

The pressure in the plate P associated with an impact velocity may be calculated by

$$P = \rho_0 D u \quad (37)$$

The density ratio  $\rho_0/\rho$  was used as a starting point so the density of the plate behind the shock wave is simply

$$\rho = \frac{\rho_0}{(\rho_0/\rho)_{\text{assumed}}} \quad (38)$$

The hydrodynamic sound speed is then approximated by taking a small increment about the pressure and calculating the slope of the equation of state. The assumption of an isentropic wave can be justified by observing that the sound speed of interest is a dilation wave relative to its very high pressure environment, behind the planar shock.

#### Pressure Increase in a Closed System

A simple calculation of the pressure increase in a box is necessary to gain insight into the amount of Al which is necessary to raise the pressure and consequently apply an impulse.

Consider a closed box of one cubic foot volume into which Al fragments are introduced suddenly. For this analysis consider the box rigid and that venting caused by the perforations are negligible. This assumption is justified the fact that the fragments causing the perforations are causing an air shock interaction at the openings which would

for the first few milliseconds of the event essentially plug the holes. The box contains initially air at standard conditions. The first law of thermodynamics for a stationary system with no external work is

$$\Delta H_a = -\delta m_p H_c \quad (39)$$

where  $\Delta H_a$  is the change of enthalpy for air between the initial and final states,  $\delta m_p$  is the mass of Al burned in air with a heat of combustion,  $H_c$ . Substituting the definition of specific heat at constant pressure  $C_{p_a}$  gives

$$(\rho_a C_{p_a} T_a)_2 - (\rho_a C_{p_a} T_a)_1 = -\delta m_p H_c \quad (40)$$

assuming a constant specific heat for air and an ideal gas at constant volume gives

$$\Delta P = - \frac{\delta m_p H_c R}{C_{p_a}} \quad (41)$$

Some justification is required for the ideal gas assumption used in this analysis. The first reason of course is the fact that it is the air in the box which is being heated and compressed. The second reason is that a detailed model of a similar situation was constructed assuming a statistical-mechanical model of the gas (Ref 3:103) with the result that the exact solutions differed only a few percent from that assuming ideal gases and neglecting intermediate products.

Figure 21 represents the increase in pressure per cubic foot of an air filled box as a function of the amount of Al

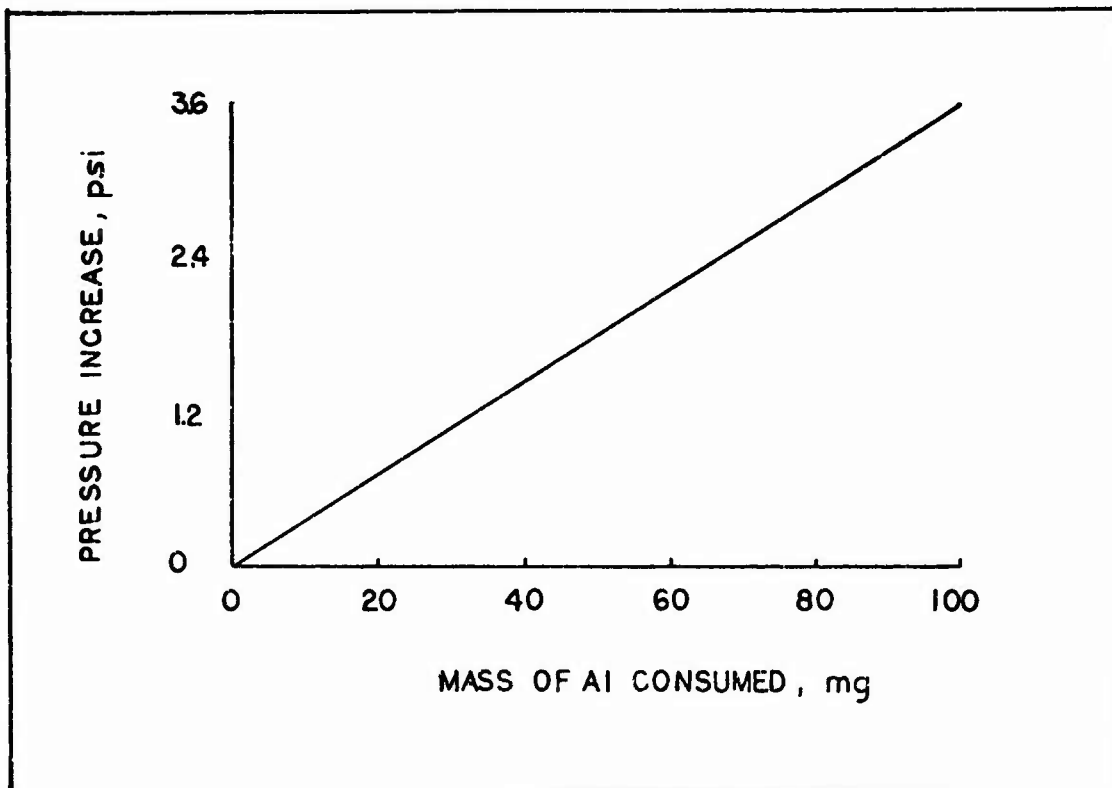


Fig 21. Pressure Change per Milligram of Al Oxidized in a One Cubic Foot Volume.

consumed by oxidation.

#### Other Design Considerations

The mechanism for sudden pressure increase is a very complex combination of different phenomena each contributing to some portion of the synergistic damage event. To analytically prescribe design criteria would be a formidable task, at least. It is clear that the formation of numerous microscopic-size high-velocity secondary fragments is essential and that above 8000 ft/sec for these microscopic fragments, combustion is almost a certainty. As shown in Figure 21, a very small amount of Al, or other pyrophoric metal, can create significant pressure increase in a small box.

It is believed that great caution must be observed before attempting to apply this phenomenon as a damage mechanism for two basic reasons. First, if the volume enclosed behind the leading, or punctured plate, is large enough that numerous sources of secondary fragments must be generated, which implies that a high area density of impacting fragments is required. The amount would vary with the volume geometry. Secondly, if the energy released by the combustion of secondary fragments is considered to be deposited in very short time at a point and that Taylor's strong blast wave theory applies, then the damage impulse will be attenuated as  $R^{-3}$ , where R is the distance from the edge of the energy source. Again there is cause for great attenuation of a shock wave generated by the impact.

For the above two reasons, and confirmed by experimental evidence for explosive oxidations (Ref 3:94) at much higher velocities, one would not seek to protect the box by inserting passive energy absorbing material as it will only serve to contain the free expansion of the combustion gases.

#### IV. Conclusions and Recommendations

##### Cause of Synergistic Damage Mechanism

The fact that there will be an explosive oxidation following a hypervelocity impact is well known (Ref 3). But the impact phenomena occurring at intermediate velocities is very much more complex. The cause of pressure build-up in a box can be attributed to several factors, any or all occurring simultaneously. One thing is reasonably clear however. The formation of numerous high-velocity microscopic-sized secondary fragments is essential for any substantial pressure increase. If the secondary particles are very small and have a velocity approximately 8000 ft/sec then, for aluminum, at least, some or all will react with the available oxygen in the system releasing additional energy.

Several sources have reported significant increases in the pressure beginning with an impact velocity of approximately 8000 ft/sec. This is because several coincidences occur simultaneously when a particle moves through air at that velocity. They are:

- (1) Stagnation temperatures around the fragment are just above the melting point of  $\text{Al}_2\text{O}_3$ ; which
- (2) allows reaction of atomic oxygen with the molten Al. Significant dissociation of  $\text{O}_2$  begins at 8000 ft/sec.

- (3) At approximately 8000 ft/sec there is sufficient heat transfer for microscopic sized fragments to overcome any chemical threshold which may exist; and
- (4) at approximately 8000 ft/sec for most experimental sized plates and projectiles, the Heyda plug-shattering model predicts that a source of these high-velocity microscopic-sized fragments is probable.

#### Application of the Synergistic Damage Mechanism

The combustion of high velocity secondary fragments following a moderately high velocity impact event has the capability to suddenly increase the pressure within the box. The conditions which are necessary are restrictive in that not every impact event will cause a secondary explosion. Basically only small, flat projectiles, which do not have ideal ballistic characteristics, will produce the necessary secondary particles which are necessary for the effect to occur. The volume of the box has an important effect on the amount of damage expected.

Should one want to build a weapon relying on secondary damage as a kill mechanism there would be, at this level of understanding, definite limitations on the confidence he would have that a kill would occur. Offense conservative criteria, that is the ability to predict confidently a

level of damage, would lead one to more predictable kill phenomena such as penetration or blast overpressure.

It is recommended that, until a comprehensive test program is conducted, the synergistic damage mechanism be treated as just that, a decided but unpredictable enhancement of known damage mechanisms.

#### Future Activity

Future efforts to understand this damage mechanism should be based on two primary objectives.

First, confirmation through a systematic test program of the Heyda plug-shattering model is required. Empirical data which would confirm or deny the existence of plug-shattering is scarce and what is available was gathered for other purposes. An extension of the model to spherical projectiles was proposed. This extension must be validated for other structural materials than aluminum.

As a corollary to this work, further analytical work on the effect of spacing of multiple fragments on a plate is necessary to develop additional mechanisms for the generation of high-velocity secondary fragments.

A second area of investigation would involve the determination of the particle size and velocity of the secondary fragments emerging from the impact event. In this study, only heuristic arguments could be presented on the determination of the size and velocity of the particles following the convergence of rarefaction waves in the plug.

This investigation would logically be a part of the verification of the Heyda model verification.

APPENDIX A

Sample Calculations

Application of Heyda Plug-Shattering Model for Calculation  
of Impact Velocity for Incipient Shattering

For test data reported in AFATL-TR-70-112 (Ref 8:146)

Plate Thickness, T: .635 in, Steel

Projectile radius, R: .391 in, Steel

The critical condition for incipient plug-shattering is

$$S = T/R \quad (21)$$

$$S = .635 / .391 = 1.624$$

From Fig 5, for steel, when  $S = 1.624$ ,  $\rho_o/\rho = .902$

The particle velocity,  $u$ , in the plate is

$$u = \frac{A}{\frac{1}{1-\rho_o/\rho} - B} \quad (24)$$

The critical impact velocity,  $\bar{V}_o$  is

$$\bar{V}_o = u + \frac{1}{2B} \left[ \sqrt{\bar{A}^2 + \frac{4B\rho_o}{\bar{\rho}} u(A + Bu)} - \bar{A} \right] \quad (26)$$

For like-material impact equation (26) simplifies to

$$\bar{V}_o = u + \frac{1}{2B} \left[ \sqrt{A^2 + 4ABu + 4B^2u^2} - A \right] \quad (26a)$$

From AFWL-TR-69-38 (Ref 10:79), values for constant A and

B are:  $A = 3.574$ ,  $B = 1.920$

Then  $u = .3993$  cm/ $\mu$ sec, from equation 24

and from equation 26a,

$$\bar{V}_o = .7986 \quad \text{cm}/\mu\text{sec} = 2619 \text{ ft/sec.}$$

Prediction of Incipient Shattering by Heyda Plug-Shattering  
Model for a Spherical Projectile

From test data reported in Hopkins, Lee and Swift (Ref 13: 343)

Plate Thickness, T: 0.787 mm, 6061-T6 Al

Projectile diameter, d: 3.17 mm, Aluminum,

From Fig 8, for incipient shattering, let  $\bar{V}_0 = 3.0$  Km/sec

Values for constants are from Ref 16:25.

$$A = .5041$$

$$B = 1.420$$

$$\rho = 2.833 \text{ gm/cc}$$

If the projectile were cylindrical the parameter S which is equal to  $T/R$  for incipient shattering is

$$S = T/R = \frac{.787}{1.585} = .497$$

Since there is no value for S as low as 0.497 and experience indicates that  $\rho/\rho$  is usually between 0.75 and 0.9 with a corresponding S approximately 1.6, the approach will be to find an equivalent  $R^*$ . If the ratio  $\frac{R^*}{R}$  is approximately constant for several geometries of impact, then hypothesize a corrective factor.

The solution procedure is to substitute values into equation 26a and solve for the target particle velocity .

$$\bar{V}_0 = u + \frac{1}{2B} \left[ \sqrt{A^2 + 4ABu + 4B^2u^2} - A \right] \quad (26a)$$

$$3.0 = u + \frac{1}{2(1.420)} \left[ \sqrt{(5.041)^2 + 4(1.420)u(5.041 + 1.420u)} - 5.041 \right]$$

which yields

$$u = 1.529 \text{ Km/sec.}$$

From equation 24, solving for ratio  $\frac{\rho_0}{\rho}$ ,

$$\frac{\rho_0}{\rho} = 1 - \frac{u}{A + Bu} \quad (24)$$

Substituting values,

$$\frac{\rho_0}{\rho} = 1 - \frac{1.59}{5.041 + (1.420)(1.529)}$$

$$\frac{\rho_0}{\rho} = .791$$

Referring to Fig 5, the associated S is 1.65.

For incipient shatter

$$S = \frac{T}{R^*}$$

$$R^* = \frac{.787}{1.65} = .477$$

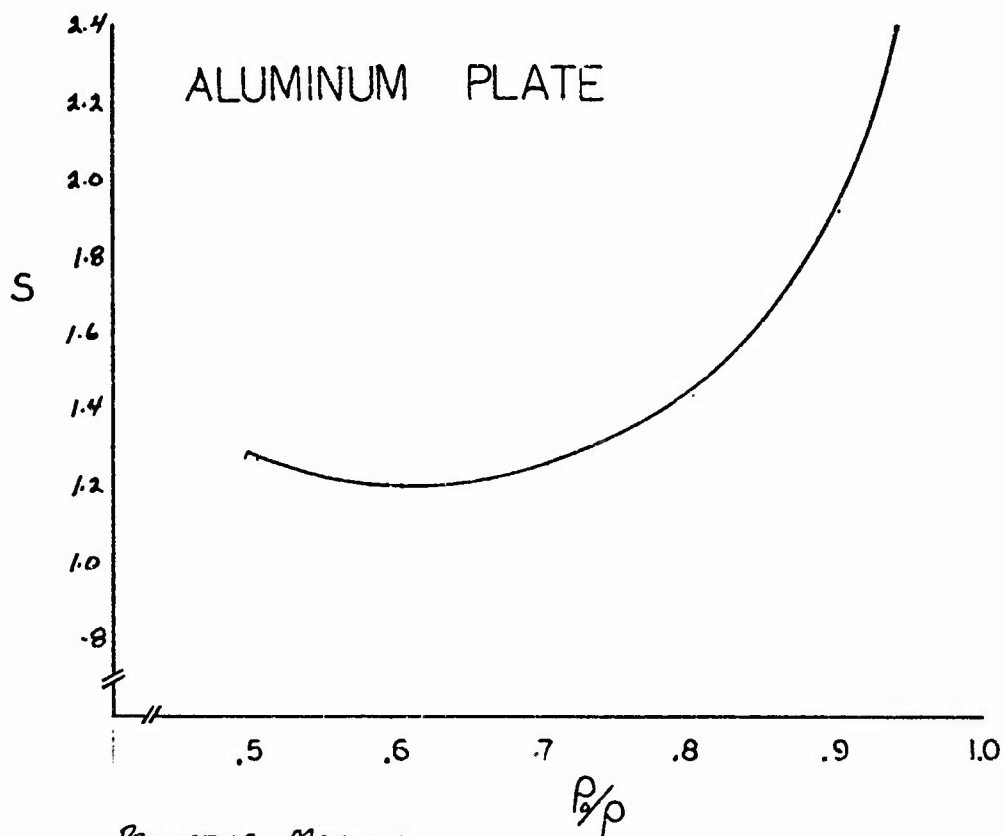
The ratio  $\frac{R^*}{R} = \frac{.477}{1.585} = .30$

APPENDIX B

Charts Required for Application of The  
Heyda Plug-Shattering Model

The following charts present the values of the parameter  $S$  as a function of the density ratio following a planar impact. When  $S$  is equal to  $T/R$ , where  $T$  is the plate thickness,  $R$  the cylindrical projectile radius incipient plug-shattering may be expected. The range of presented is believed, without experimental verification, to be the range of practical application.

The charts may be entered either through the system geometry,  $S$ , and then reading directly the density ratio. The curve represents only the plate material. Below the chart the velocity at impact of a variety projectile materials is presented.



PROJECTILE MATERIAL  
IMPACT VELOCITY, ft/sec

STAINLESS STEEL

40213 22629 12995 6970 2978 0

TUNGSTEN

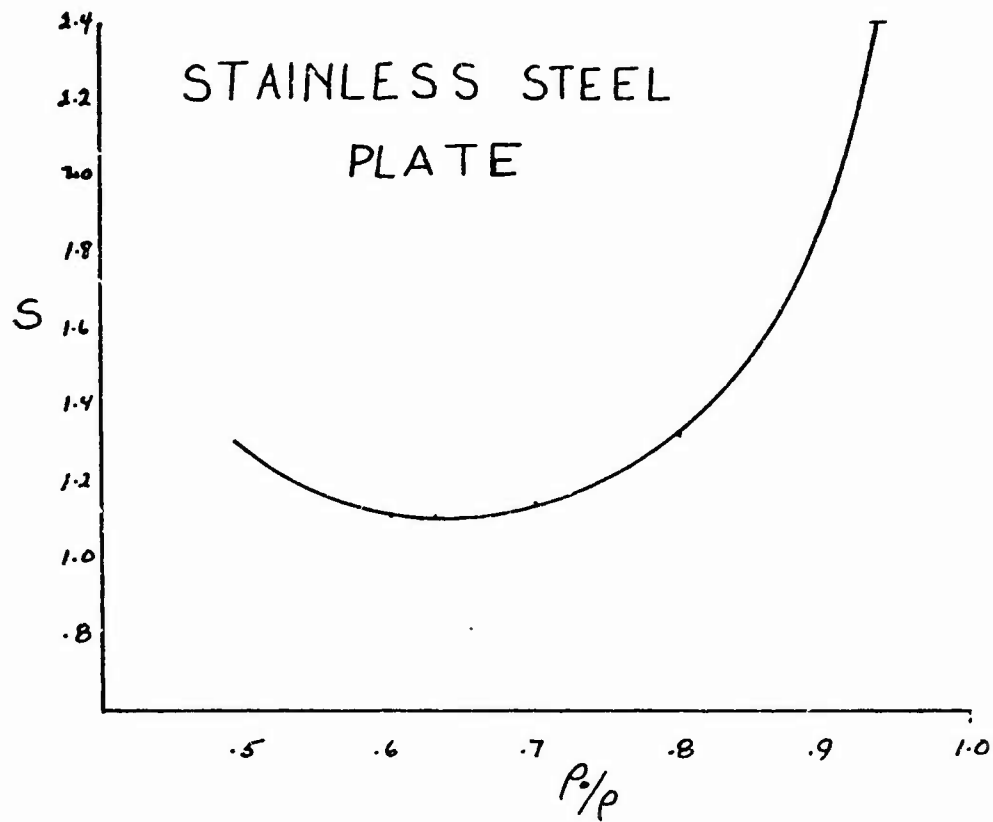
34899 19431 11063 5901 2487 0

LEAD

41656 22753 13402 7413 3198 0

ALUMINUM

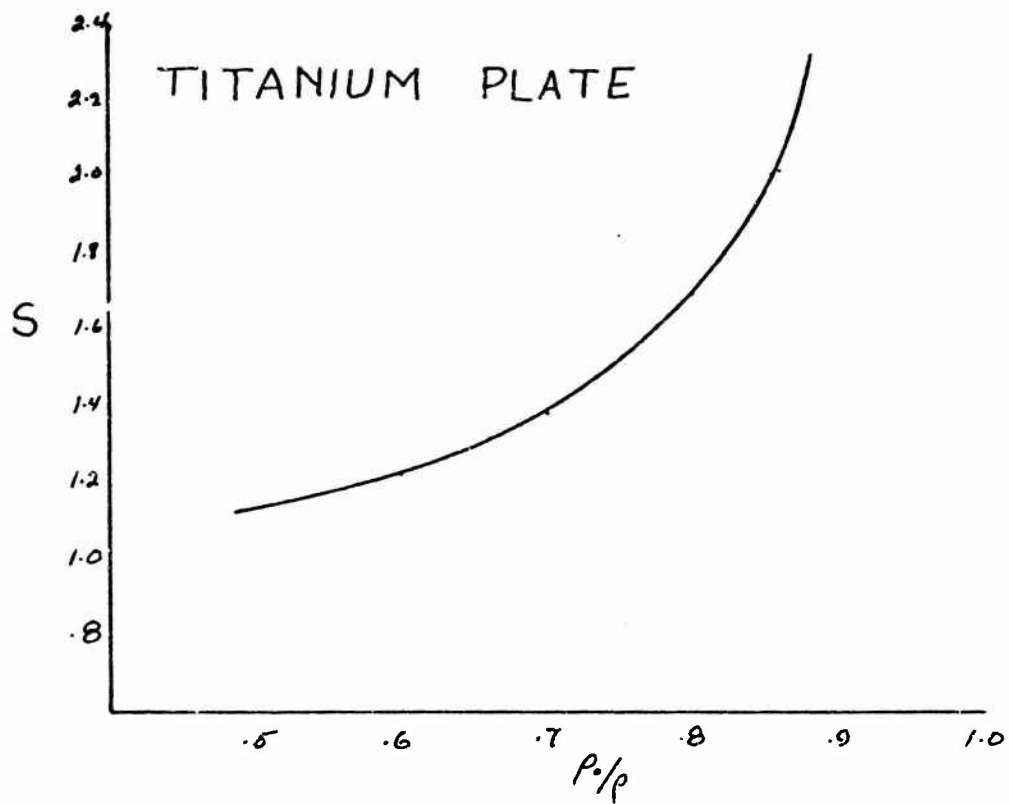
52808 30078 17515 9545 4034 0



PROJECTILE MATERIAL  
IMPACT VELOCITY, ft/Sec

STAINLESS STEEL  
58187      29520      16216      2528      3519      0

TUNGSTEN  
48085      23911      12825      6593      2650      0



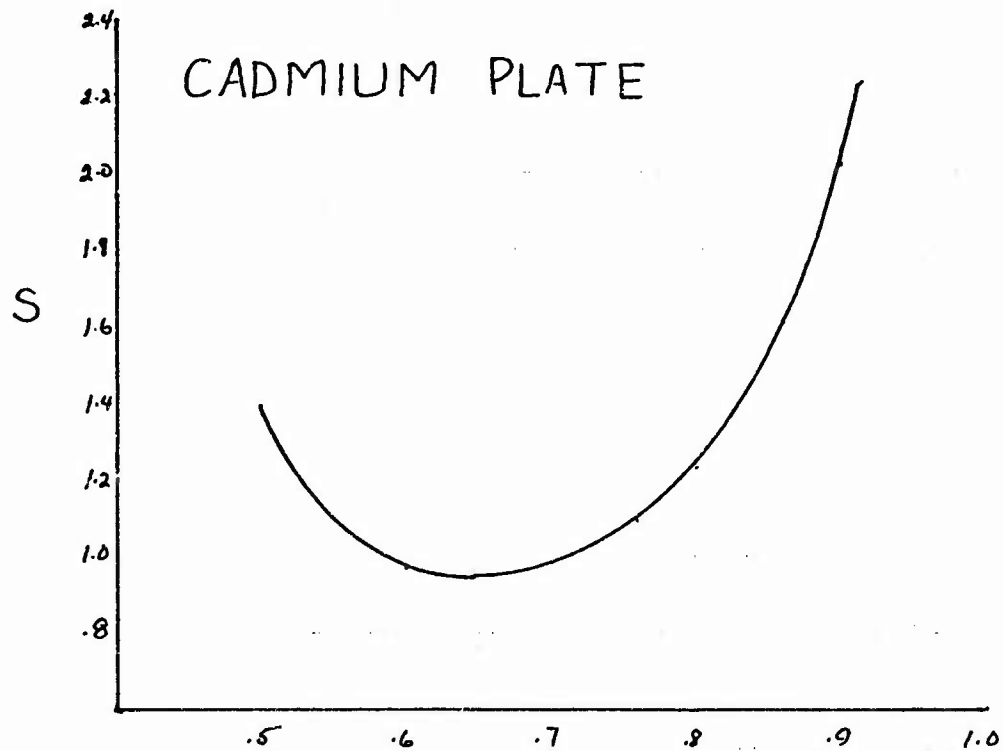
PROJECTILE MATERIAL  
IMPACT VELOCITY, ft/sec

TUNGSTEN

23157	14990	9381	5346	2329	0
-------	-------	------	------	------	---

TITANIUM

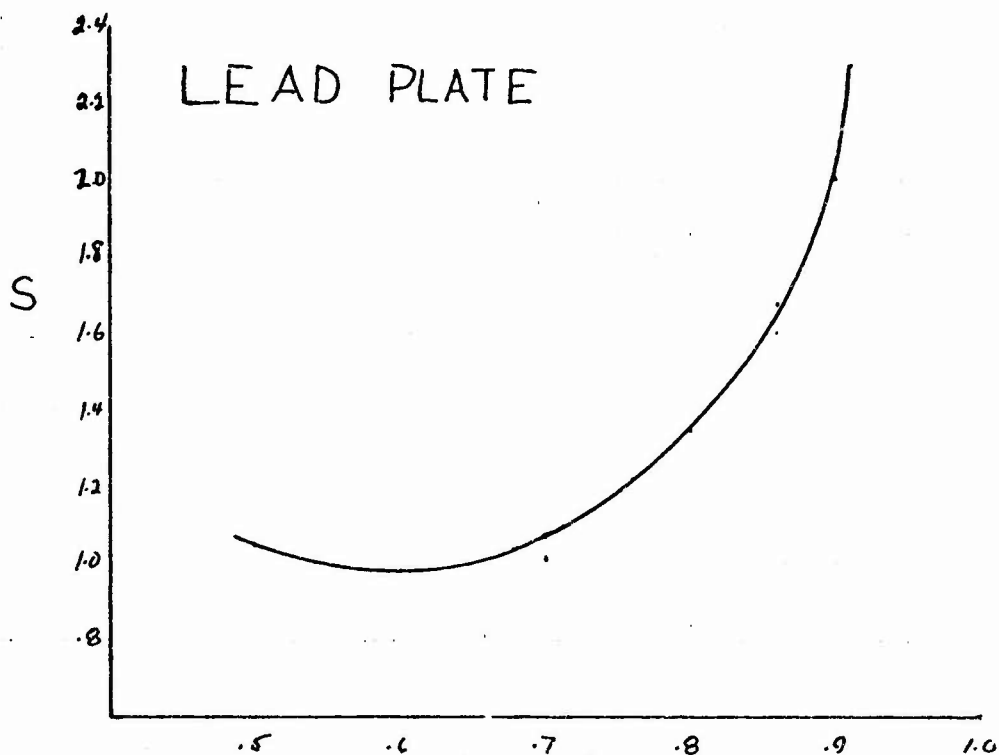
33653	22042	14006	8102	3575	0
-------	-------	-------	------	------	---



PROJECTILE MATERIAL  
 IMPACT VELOCITY, ft/sec

CADMIUM

Impact Velocity (ft/sec)	S
48872	1.4
19198	1.0
9643	0.95
4922	1.0
1938	2.2
0	



PROJECTILE MATERIAL  
IMPACT VELOCITY, ft/sec

LEAD

24915      12923      7193      3705      1575      0

Bibliography

1. Zandstra, T. W. Experiments to Determine the Physical Nature of Flash (Vaporific) Damage, Preliminary Report No. 3. NMSM/RDD/T-629. New Mexico School of Mines, May 1949. AD 498389.
2. Caron, A. P. Oxidative Detonations Initiated by High Velocity Impacts. AFFDL-TR-65-41. Wright-Patterson AFB, Ohio: Air Force Flight Dynamics Laboratory, May 1965. AD466558.
3. Friend, W. H. et al. An Investigation of Explosive Oxidations Initiated by Hypervelocity Impacts. AFFDL-TR-67-92. Wright-Patterson AFB, Ohio: Air Force Flight Dynamics Laboratory, August 1967. AD821326.
4. Backman, M. E. and W. J. Stronge. Penetration Mechanics and Post-Perforation Effects in an Aluminum - Aluminum Impact System. NWC TP 4414. China Lake, California; Naval Weapons Center, October 1967. AD661833.
5. Miklowitz, Julius. "Plane-Stresses Unloading Waves Emanating From a Suddenly Punched Hole in a Stretched Elastic Plate." Journal of Applied Mechanics, Trans. of ASME, December 1960.
6. Rinehart, J. S. and John Pearson. Behavior of Metals Under Impulsive Loads. New York: Dover Publications, 1954.
7. Cook, Melvin A. The Science of High Explosives. New York: Reinhold Book Corporation, 1958.
8. Woodall, S. R., J. F. Heyda, and H. J. Galbraith. Ballistic Impact Mechanics of Selected Metallic and Composite Materials, Book I and II. AFATL-TR-70-112. Eglin Air Force Base, Florida: Air Force Armament Laboratory, November 1970. AD891958.
9. Kohn, B. J., Compilation of Hugoniot Equations of State. AFWL-TR-69-38. Kirtland Air Force Base: Air Force Weapons Laboratory, April 1969. AD852300.
10. Swift, H. F. "Hypervelocity Impact" in Dynamic Response of Materials to Intense Impulsive Loadings, edited by P. C. Chow and A. K. Hopkins. Wright-Patterson Air Force Base, Ohio: Air Force Materials Laboratory, 1973.

11. Riney, T. D. "Numerical Evaluation of Hypervelocity Impact Phenomena" in High-Velocity Impact Phenomena edited by Ray Kinslow. New York, New York: Academic Press, 1970.
12. Hopkins, A. K., T. W. Lee, and H. F. Swift. "Material Phase Transformation Effects upon Performance of Spaced Bumper Systems." Journal of Spacecraft and Rockets, Vol. 9, No. 5, May 1972.
13. Cox, R. N. and L. F. Crabtree. Elements of Hypersonic Aerodynamics. New York: Academic Press, 1965.
14. Richardson, F. D. and J. H. E. Jeffes, "Standard Free Energy of Formation of Oxides as a Function of Temperature." J. Iron and Steel Inst., 160, 261, 1948. Modified by L. S. Darken and R. W. Gurry, Physical Chemistry of Metals. New York: McGraw-Hill, 1953.
15. Morrison, Richard B., editor. Design Data for Aeronautics and Astronautics. New York: John Wiley, 1962.
16. Williams, Forman A. Combustion Theory. Reading, Massachusetts: Addison-Wesley, 1965.
17. Hansen, C., Frederick and Steve P. Heims. A Review of the Thermodynamic, Transport, and Chemical Reaction Rate Properties of High-Temperature Air. NACA TN 4359, Moffett Field, California: Ames Aero Lab, July 1958.
18. Friedman, R. and A. Macek. "Ignition and Combustion of Aluminum Particles in Hot Ambient Gases." Combustion and Flame, VI:9-19 (March 1962).
19. Balyaev, A. F., Yu. V. Fralov, A. I. Korotkov, "Combustion and Ignition of Particles of Finely Dispersed Aluminum." Fizika Goreniya i Vzryva, Vol. 4, No. 3, 1968.

Vita

Russell Thompson Boice, Jr. was born [REDACTED] in [REDACTED] [REDACTED] He graduated from the [REDACTED], Philadelphia in 1952, attended Drexel Institute of Technology until entering the USAF Aviation Cadet Program in 1954. He graduated from pilot training and received his commission in February 1956. He served as an instructor pilot in the 3500th Pilot Training Squadron, Reese AFB, Texas and as an KC-97 Aircraft Commander with the 509th Air Refueling Squadron, Pease AFB, New Hampshire until entering the University of Wyoming in 1965.

He graduated from there with a Bachelor of Science in Mechanical Engineering degree and was elected to Phi Kappa Phi and Sigma Tau. He served in Southeast Asia with the 12th Special Operations Squadron and 315th Special Operations Wing. He then served as Project Engineer in the Ballistic Missile Branch, Strategic Systems Division, Deputy for Development Plans, SAMSO, Norton AFB, California until May 1972. He attended the Air Force Institute of Technology where he received the degree of Master of Science in 1974.

Permanent address: [REDACTED]

[REDACTED]

This thesis was typed by [REDACTED] [REDACTED]

[REDACTED]